Analysis of the effect of principal stresses in the Charlevoix, Lower St. Lawrence, Northern Appalachian, Laurentian Slope and Grand Banks Regions on faults in Nova Scotia and New Brunswick

Ella Goldberg

Submitted in partial fulfillment of the requirements
for the degree of Bachelor of Science, Honours
Department of Earth Science
Dalhousie University, Halifax, Nova Scotia
March 2012

Distribution License

DalSpace requires agreement to this non-exclusive distribution license before your item can appear on DalSpace.

NON-EXCLUSIVE DISTRIBUTION LICENSE

You (the author(s) or copyright owner) grant to Dalhousie University the non-exclusive right to reproduce and distribute your submission worldwide in any medium.

You agree that Dalhousie University may, without changing the content, reformat the submission for the purpose of preservation.

You also agree that Dalhousie University may keep more than one copy of this submission for purposes of security, back-up and preservation.

You agree that the submission is your original work, and that you have the right to grant the rights contained in this license. You also agree that your submission does not, to the best of your knowledge, infringe upon anyone's copyright.

If the submission contains material for which you do not hold copyright, you agree that you have obtained the unrestricted permission of the copyright owner to grant Dalhousie University the rights required by this license, and that such third-party owned material is clearly identified and acknowledged within the text or content of the submission.

If the submission is based upon work that has been sponsored or supported by an agency or organization other than Dalhousie University, you assert that you have fulfilled any right of review or other obligations required by such contract or agreement.

Dalhousie University will clearly identify your name(s) as the author(s) or owner(s) of the submission, and will not make any alteration to the content of the files that you have submitted.

If you have questions regarding this license please contact the repository manager at dalspace@dal.ca.

Grant the distribution license by signing and dating below.

_____ _____

Name of signatory Date

Department of Earth Sciences
Halifax, Nova Scotia
Canada B3H 4J1
(902) 494-2358
FAX (902) 494-6889

DATE: March 19th, 2012

AUTHOR: Ella Goldberg

TITLE: ANALYSIS OF THE EFFECT OF PRINCIPLE STRESSES IN THE CHARLEVOIX, LOWER ST. LAWRENCE, NORTHERN APPALACHIAN, LAURENTIAN SLOPE AND GRAND BANKS REGIONS ON FAULTS IN NOVA SCOTIA AND NEW BRUNSWICK

Degree: B.Sc. Hons. Convocation: May Year: 2012

Abstract

Stress patterns were analyzed in parts of Atlantic Canada to determine the tectonic regimes and whether reactivation of older faults could cause damage near Point Lepreau, New Brunswick. Point Lepreau is home to a nuclear power plant and seismic risk information in the Northern Appalachians is scarce and out of date. To put this information in perspective regionally, the study area extends from south of Grand Manan Island in the southwest to the Grand Banks of Newfoundland in the northeast.

This study investigated published focal mechanism data for earthquakes from ~1970 to 2011 in the study area. Five main regions of seismicity are the Northern Appalachians, Charlevoix, Lower St. Lawrence, offshore Nova Scotia and the Grand Banks. Earthquake and focal mechanism data were obtained from the Global Centroid Moment Tensor Catalogue (1976-present), the Canadian Earthquake Database, and the U.S. Geological Survey/ National Earthquake Information Centre database (1973-present) and focal mechanism data from several Geological Survey of Canada open files. Focal mechanism information is scarce for most regions. In order to better characterize the principal stress pattern for the regions, the World Stress Map Data (2008) were included in the study. The only event that had a known fault plan was the 1929 Mn= 7.2 Laurentian Slope event that caused a submarine slump which then induced a tsunami (Bent, 1995).

Analysis of focal mechanisms showed thrust-fault stress regime in the Gulf of St. Lawrence with three clusters of principle compressive stress axes where two clusters are separated by the St. Lawrence fault. Some of the Northern Appalachian's focal mechanisms show strike-slip stress regime. Between the Bay of Fundy and the Gulf of St. Lawrence, World Stress Map data show thrust faulting with a strike-slip component closer to the Northern Appalachians and pure thrust faulting closer to the Gulf of St. Lawrence. In the Grand Banks region, stress orientations seem random and the cause of earthquakes is unknown. Offshore Nova Scotia, the stress orientations seem to coincide with the trend for North America and are compatible with the extension perpendicular to the passive Atlantic boundary.

Shear stress on two major faults was calculated; the St. Lawrence Fault in the Charlevoix region and the Oak Bay fault in the Northern Appalachian region. The shear stress on the Oak Bay fault was found to be very small and reactivation is unlikely while some faults in the Charlevoix region are oriented the same as the St. Lawrence fault; indicating that reactivation happens occasionally.

In summary; the Oak Bay fault is an unlikely threat to Point Lepreau's nuclear power plant, the Charlevoix region's St. Lawrence fault is active but the largest threat to Point Lepreau are earthquake-induced tsunamis or earthquake-induced landslides that can generate tsunamis in the Laurentian Slope zone.

Table of Contents

Table of Figures

List of Tables

Acknowledgements

I would like to thank my fellow classmates, the Dawson Geology club, and the faculty and staff of Dalhousie's Earth Science Department for their infallible support and aid over the past four years. I am also grateful to Grant Wach for the use of the Basin Lab and Charlie Walls for his help with research. I am much appreciative of the encouragement and helping hand of Martin Gibling, Mike Young, Kyle Langille, and my close friends along the way. Finally, I would like to thank my supervisor, Djordje Grujic, for sharing with me his wealth of knowledge about structural geology and for the opportunity to study such an interesting and challenging topic. It has been an incredible learning experience. Thank you!

1.0 Introduction

1.1 Purpose and motivation

The purpose of this study is to analyse the principal stresses from historical earthquakes near Point Lepreau, New Brunswick (Figure 1.1) to determine their potential seismic risk at the nuclear generating station in Point Lepreau. On March 11 2011, the magnitude 9.0 (Mw) earthquake off the coast of Tōhoku, Japan, caused a tsunami which flooded the Fukushima power plant causing failure of the cooling system. Failure of the cooling system led to the overheating of the Uranium fuel rods, which caused the cooling water to split into hydrogen and oxygen and eventually the hydrogen exploded (Sample, 2011). Radiation levels at the boundary of the plant are said to have reached a quarter of the annual background radiation following the meltdown and tap water and soils were also polluted (Sample, 2011). The aftermath of the Fukushima incident sparked interest in the safety of other nuclear generating stations around the world, in particular those located in coastal areas. This study was motivated by the Sierra Club's concern in the safety of the Point Lepreau Nuclear Generating station.

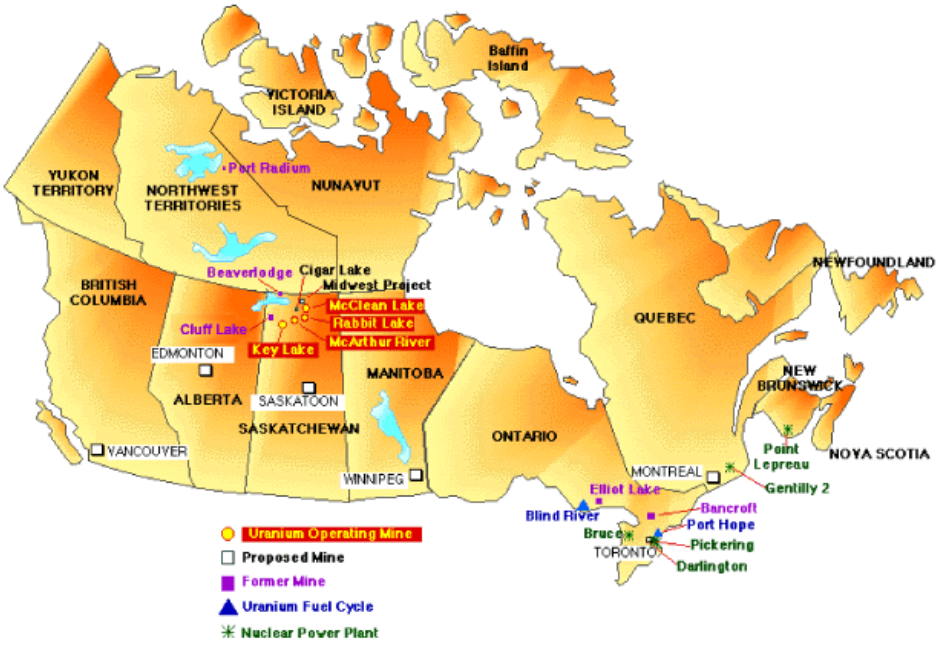

Figure 1.1: Map of Canada showing nuclear generating stations, including Point Lepreau (After World Nuclear Association, 2012).

The scope of this project was to collect data from earthquake databases to determine the focal mechanisms of earthquakes and calculate the regional seismic kinematics and seismic strain. This was done through compiling published data, mapping focal mechanism solutions and analysing the regional and local stress patterns. Following the definition of the GSC, five seismic regions have been analysed: the Lower St. Lawrence (LSL), the Charlevoix region of the St. Lawrence (CHV), Northern Appalachian region (NAP), Offshore Nova Scotia and Laurentian Slope (LSP), and the Grand Banks (Figure 1.2). The LSL and CHV zones lie within the St. Lawrence Rift system.

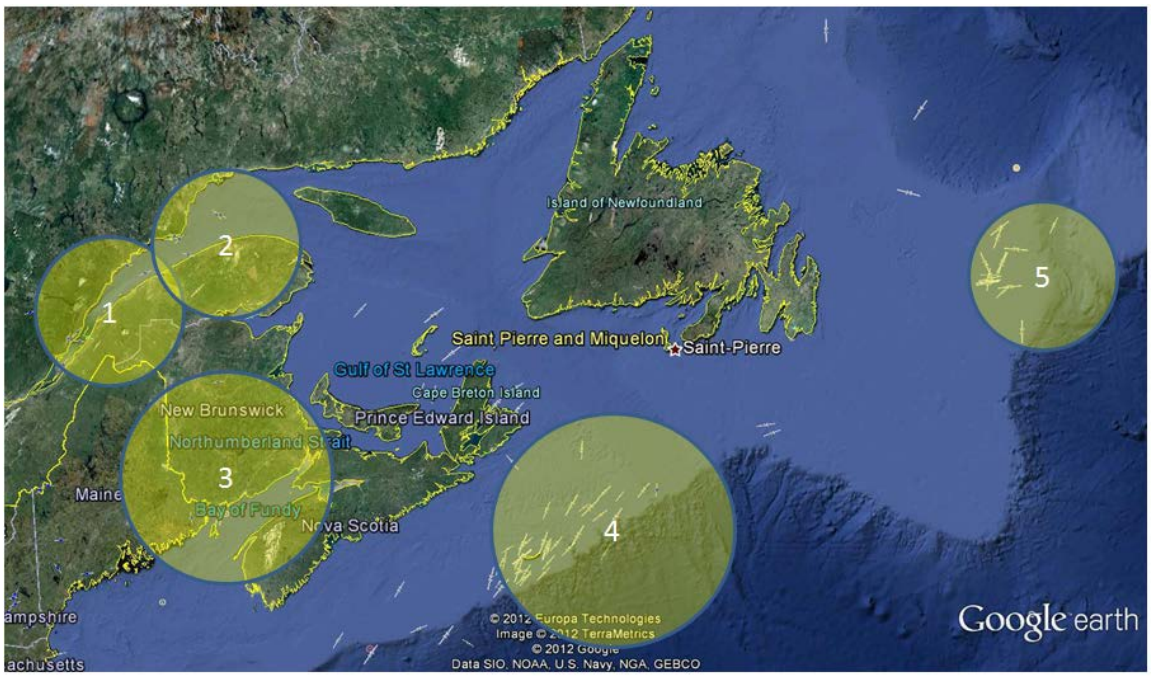

Figure 1.2: Seismotectonic areas of southeastern Canada and the regional crustal stress pattern. (1) Charlevoix region of the St. Lawrence, (2) the Lower St. Lawrence, (3) Northern

Appalachian, (4) Offshore Nova Scotia and Laurentian Slope, (5) the Grand Banks. Image taken using Google Earth Pro.

There are two faults in the Point Lepreau area of the Bay of Fundy that are of interest to this study; the Cobequid-Chedabucto fault zone (CCFZ) and the Oak Bay fault. These two faults may contribute to the approximate 5000 earthquakes that are documented within the study area from 1568 until 2011 (Fig. 3).

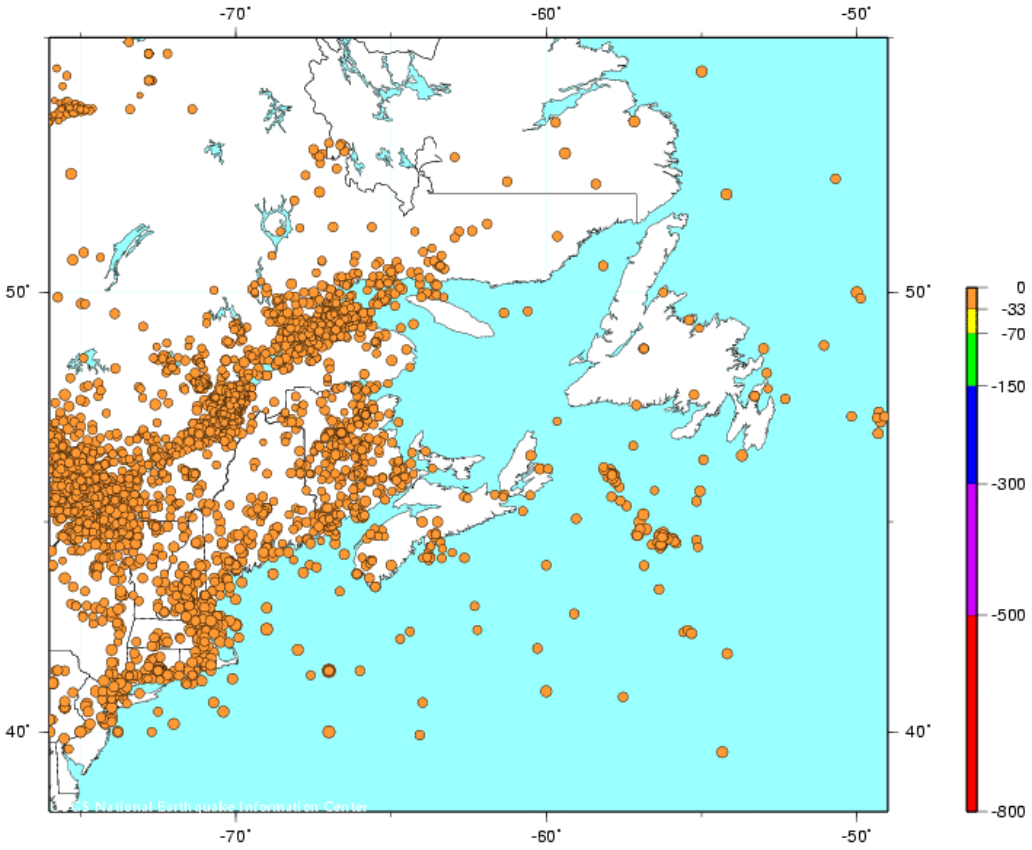

Figure 1.3: Study area showing 5388 earthquakes from 1568 to 2011. Data compiled from Canada's National Earthquake Database (http://earthquake.usgs.gov/earthquakes/eqarchives/epic/epic_rect.php)

Other, more likely sources for the earthquakes in Eastern Canada include the faults of the Saint Lawrence Rift System (SLRS). In addition, causes for seismicity could include (a) differential vertical motion due to isostatic rebound after ice sheet retreat, (b) salt tectonics or (c) submarine landslides. This study will focus on focal mechanism data, world stress map data, and vertical and horizontal global positioning system (GPS) velocity data to determine principal stresses and calculate the stress and strain the Oak Bay fault.

1.1.1 Data

The study area is situated between 38° N to 55° N latitude and 76° W to 49° W longitude and extends from Newfoundland to New Brunswick and to southern Quebec (Fig. 1.2). The data for this study were retrieved mostly from GSC open files (1986-2000) and few focal solutions were retrieved from the Global Centroid Moment Tensor Catalogue. The National Earthquake Information Centre (NEIC) provided the basis to search several databases, the most important being Canada's National Earthquake database.

1.2 Regional tectonic setting and seismicity

Atlantic Canada is situated on the North American plate which, on is east coast has a passive margin. Volcanism does not occur on this passive margin, but earthquakes do. There are several sources of seismicity in and around Nova Scotia and New Brunswick. The main focus of this project will be the historical activity of the Cobequid-Chedabucto Fault system and the likelihood of its reactivation.

1.2.1 Cobequid-Chedabucto Fault System

The Cobequid-Chedabucto fault system or zone (CCFZ) extends on land for about 300 km and is estimated to stretch from the Bay of Fundy between Nova Scotia and New Brunswick to and

beyond Grand Banks, Newfoundland (Fig. 1.5). The CCFZ trends ENE-WSW and is composed of two adjoining faults, the Cobequid and the Chedabucto faults (Fig. 1.5). It runs through the Minas Basin (Fig. 1.6a) in northern Nova Scotia and is estimated to extend into the Bay of Fundy between Nova Scotia and New Brunswick. The Cobequid-Chedabucto fault system is a transpressional boundary between the Meguma and Avalon terranes (Macinnes, 2004). The CCFZ consists of a high-strain internal zone and a lower strain external zone dominated by folds (Fig. 1.4). The high strain zone is further subdivided into: marginal, core and the shear band domain (Macinnes, 2004), (Fig. 1.4). The fault zone on the east coast of Nova Scotia is characterized by ductile foliation with extension lineation defined by elongated quartz and aligned mica grains in metasediments and granitoids (Mawer & White, 1986). The S-C textures in both the granitoids and metasedimentary rocks indicate a dextral sense of shear. In the Greville Bay, brittle deformation dominates with shear sense indicators showing dextral motion as well (Mawer & White, 1986).

The fault system initiated in the early Carboniferous, when the Meguma and Avalon Terranes began to separate. There is geological evidence for a repeated slip along the CCFZ . Pe-Piper & Piper (2004) suggest that the strike slip motion of the CCFZ near Grand Banks affected the Early Cretaceous-Tertiary evolution in Atlantic Canada and that the CCFZ is part of a much larger fault system, the Newfoundland–Azores–Gibraltar fracture (Fig. 1.5). There are several geological features in Atlantic Canada that may be related to strike-slip motion along the CCFZ in the early Tertiary. These include:(1) Cretaceous Chaswood Formation basins in central Nova Scotia; (2) mid-Cretaceous unconformities on the southern Grand Banks; (3) early–mid Cretaceous offshore volcanism; (4) rapid subsidence of the eastern Scotian Basin in the mid Cretaceous; and (5) Oligocene uplift of the eastern Scotian Shelf, (Pe-Piper & Piper, 2004)

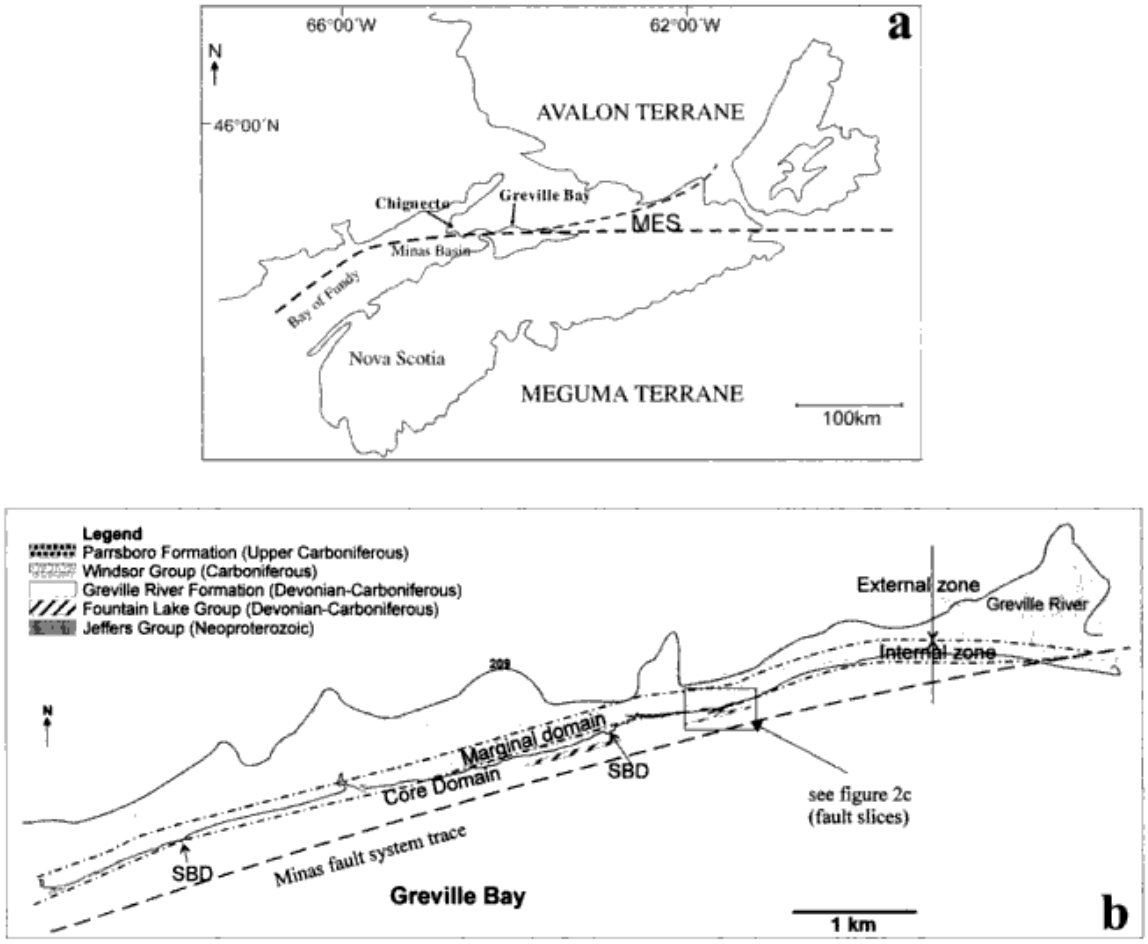

Figure 1.4: Cobequid-Chedabucto fault system (a) The Minas fault system after Macines (2004), (b) Structural zones of the fault zone in the Greville bay. High strain (internal) zone separated into the core, marginal and shear band domains. MFS: Minas Fault System; SBD: Shear band domain (Macinnes, 2004).

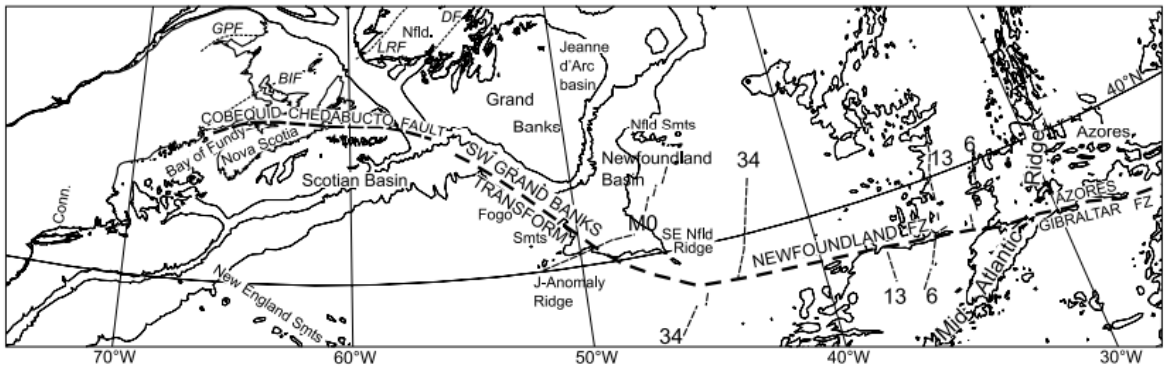

Figure 1.5: The Newfoundland–Azores–Gibraltar fracture zone and the southeastern Canadian margin. BIF, Bellisle fault; DF, Dover fault; GPF, Grand Pabos fault; LRF, Long Range fault. Conn., Connecticut; FZ, fault zone; Smts, Seamounts. (from Pe-piper & Piper, 2004)

The dextral sense of motion along the CCFZ in the Paleozoic (Mawer & White, 1986,) changed to sinistral in the Triassic- early Jurassic (Pe-Piper & Piper, 2004). The sinistral motion produced pull-apart basins along the CCFZ around the same time as the North Mountain Basalt (NMB) was extruded. Post-early Jurassic, the motion changed to reverse dip-slip during a regional NW-SE compression.

In the middle Cretaceous (Aptian–Cenomanian) dextral motion along the CCFZ created extension in the releasing bend in the Laurentian sub-basin (Fig. 1.6) resulting in rift-related volcanism occurring in the Orpheus graben followed by rapid subsidence on the Scotian margin and the SW Grand Banks margin. The Cretaceous Chaswood Formation is located in central Nova Scotia is a fluvial succession up to 200m thick. It was deposited in fault-bound basins of the same deformational phase as the Orpheus Graben, Laurentian subbasin and Jeanne d d'Arc basin, which are along the strike of the CCFZ (Pe-Piper & Piper, 2004). The Chaswood Formation shows deposition in pull-apart basins in its upper and middle members. A major unconformity of the mid-Cretaceous can be seen throughout the fault system in the Chaswood

Formation, the Orpheus Graben and on the SW Grand Banks (Fig. 1.6) (Pe-Piper & Piper, 2004). This unconformity cuts through the youngest member of the Chaswood Formation, further implying that the Cobequid-Chedabucto fault in central Nova Scotia was likely active during the Cretaceous.

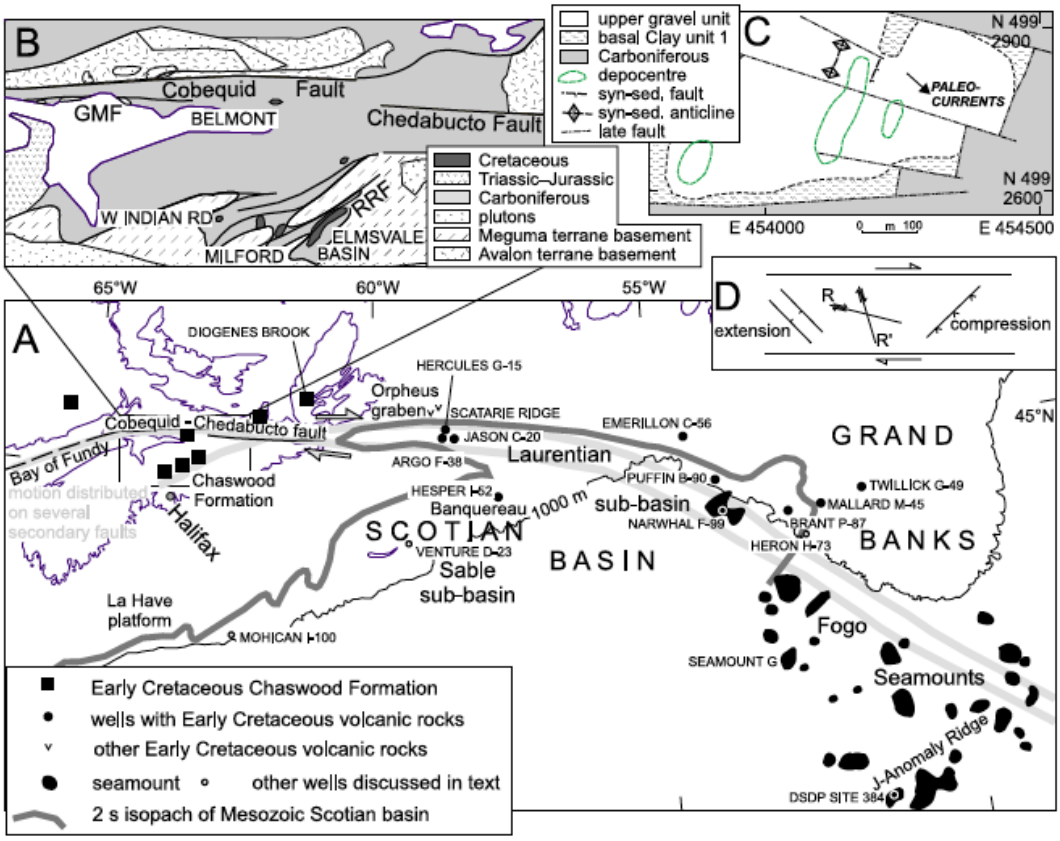

Figure 1.6: "Cretaceous Cobequid – Chedabucto – SW Grand Banks fault system in Atlantic Canada. (A) Major tectonic features (including the Laurentian Sub-basin, CCFZ, and Orpheus Graben). DSDP, Deep Sea Drilling Project. (B) Chaswood Formation and major faults of central Nova Scotia. GMF, Gerrish Mountain Fault; RRF, Rutherford Road fault. (C) Principal faults in the West Indian Road Pit. (D) Schematic diagram of secondary fault structures developed in a dextral strike-slip system. R, R′ are Riedel shears," (after Pe-Piper & Piper, 2004)

In agreement with activity in the Cretaceous along the CCFZ, it is suspected that there were two major periods of tectonic activity in the Cretaceous-Cenozoic along the CCFZ (Pe-Piper & Piper, 2004). In the Aptian to Cenomanian there was a period where spreading between Iberia and the Grand Banks was faster than spreading at the central Atlantic; this period corresponds with dextral strike slip movement along the Cobequid – Chedabucto– SW Grand Banks fault. Deformation in the Oligocene that is responsible for the uplift of the eastern Scotian Shelf can be accounted for by attributing the motion to be along the Cobequid – Chedabucto– SW Grand Banks fault (Pe-Piper & Piper, 2004). Therefore, the last inferred tectonic activity along the CCFZ was dextral strike-slip at ~34 Ma.

1.2.2 Oak Bay fault

The Oak Bay fault is northwest trending and runs from Oak Bay, NB through Passamaquoddy Bay and potentially connects to the Grand Manan fault, comprising the Grand Manan-Oak Bay Fault System (Miller et al., 2007) (Fig. 1.7). The NAP region of the study area comprises several terranes, or fault-bounded blocks including (from inboard to outboard): St. Croix, Mascarene, new River, Kingston, Brookville, Avalon, and Meguma (Fig. 1.7). Miller et al. (2007), found that the some units on Grand Manan Island show similar U-Pb (zircon) age to the Ilsesboro block (which is between the Ellsworth and St. Croix terranes (Fig. 1.7). These U-Pb (zircon) ages along with a similarity in lithology suggest that the New River and Mascarene terranes could have once been together, which implies an post-Silurian offset of ~40 km between southern New Brunswick and Maine along the Grand Manan- Oak bay fault system (Miller et al., 2007).

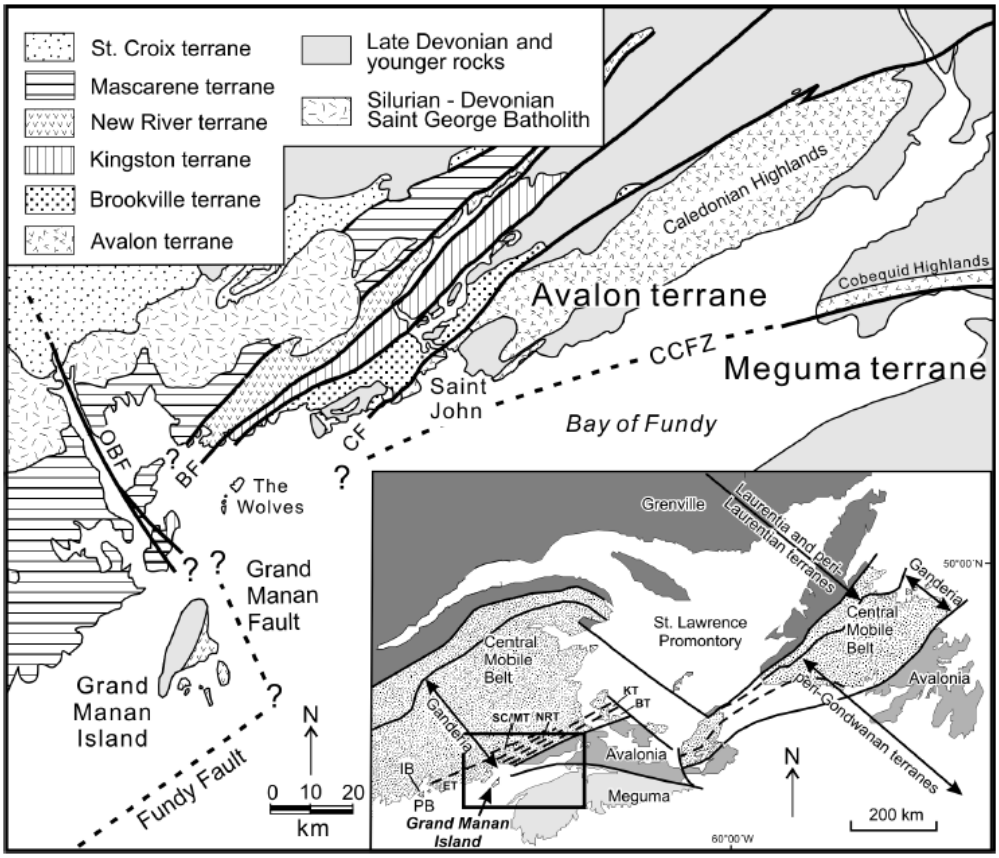

Figure 1.7: Location of the Oak Bay fault (OBF), Cobequid-Chedabucto Fault Zone (CCFZ), Bellisle fault (BF), Caledonia fault (CF) in context of terranes in the NAP seismic zone. Inset shows major tectonic domains of northern Appalachian Orogen; Brookeville terrane (BT), Ellsworth terrane (ET), Isleboro block (IB), Kingston terrane (KT), New River terrane (NRT), Penobscot Bay (PB), and St. Croix and Mascarene terranes (SC/MT). After Miller et al. (2007).

Several epicentres of recent earthquakes are near the Oak Bay fault (Fig. 1.3), which causes concern as to the fault's motion in recent times. However, an undeformed Triassic dyke that transects the Oak Bay fault, suggests that there has been no movement along the Oak Bay Fault since at least the Triassic and glacial striations at 24 locations do not show signs of activity along the fault in the Quaternary either (Natural Resources Canada, 2011). However, pockmarks on

the bottom of Passamaquoddy Bay (Fig. 1.8) with a northwestern alignment may be an indicator of potential movement along northwest-trending faults such as the Oak Bay fault as movement along a fault could cause methane release, and therefore pockmarks (Wildish et al., 2008). An alternative explanation is that the pockmarks were created by gas release due to subsidence of Passamaquoddy Bay (Natural Resources Canada, 2011).

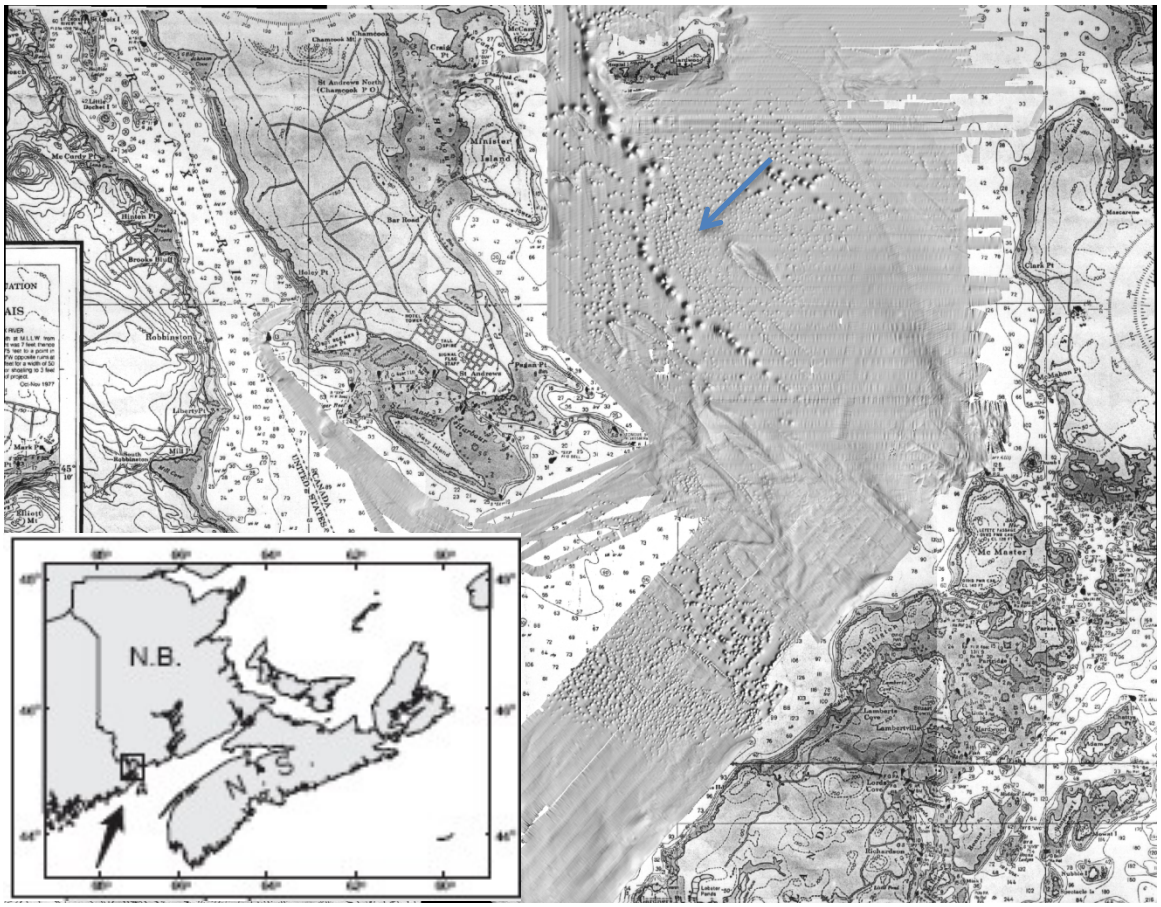

Figure 1.8: Multibeam image of pockmarks in Passamaquoddy Bay showing northwestern alignment of pockmarks (indicated by blue arrow). Inset shows the location of Passamaquoddy Bay in relation to Nova Scotia and New Brunswick. After Wildish et al. (2008).

1.2.3 Saint Lawrence Rift system

The Saint Lawrence Rift system is comprised of late Proterozoic Iapetus Rift structures. The main faults are the St. Lawrence and Cap-Tourmente faults. The St. Lawrence fault strikes NE-

SW and dips 60° - 70° SE and the Cap-Tourmente fault strikes east and dips steeply (~80°) south. Both faults are normal and run through the St. Lawrence Gulf. The LSL and CHV seismic zones lie along the main Iapetus Rift structures; the St. Lawrence fault separating the CHV and some of the LSL zone into its hanging wall and footwall (Fig. 1.9) while the NAP region does not seem to be associated with any structures on a lithospheric scale (Mazzotti & Townend, 2010).

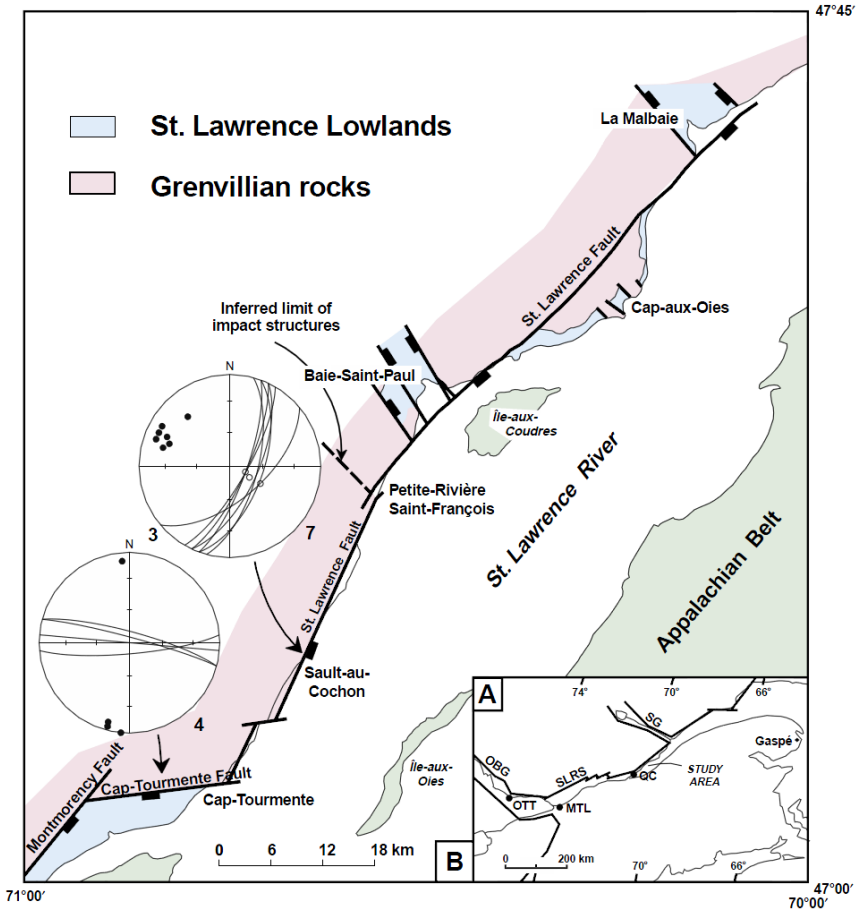

Figure 1.9: Charlevoix region showing faults associated with the St. Lawrence Rift system; most notably, the St. Lawrence fault, Montmorency fault and Cap-Tourmente fault. These faults separate the Northeast shore (footwall) region from the base of the river in the southwest (hanging wall) (After Tremblay & Lemieux, 2001).

The Saint Lawrence Rift structures have significance for this study as both the Charlevoix and Lower St. Lawrence zones are located along the main Iapetus Rift structure and also because the Northern Appalachian region does not seem to be associated with the main or subsequent failed rift arms. Fault structures along the St. Lawrence and Cap-Tourmente are very similar and include fault breccia, cataclasites, foliated fault gouges, pseudotachylite, and C/S fabrics and shear bands in ultracataclasites that clearly indicate a normal sense of faulting (Tremblay & Lemieux, 2001). It is believed that the Montmorency fault and the St. Lawrence fault developed from en echelon faulting and that the Cap-Tourmente fault is a transfer fault (Tremblay & Lemieux, 2001). Preliminary apatite fission-track ages of basement rocks that fringe the Montmorency Fault and cross cutting relationships indicate that the faults were activated in the late Devonian or younger and therefore are thought to be concurrent with the opening of the Atlantic Ocean in the Mesozoic (Tremblay & Lemieux, 2001).

1.2.4 Earthquakes

East of Ottawa (and east of 75°W) about 5000 earthquakes were registered from 1568 until January 1, 2012 (Fig. 1.3). However, only a small percentage has a known focal mechanism, which, without dense seismographs requires a Mn ≥ 5 (Smith, R.B). The focal mechanisms were reported in a series of Open Files up to 2000 and the only known recent studies are for the Saint Lawrence and Charlevoix however no regional study is known for the study area shown in figure 1.2. There are also several papers about the 1929 and 1975 earthquake in the Laurentian channel. In this study, data from focal mechanisms for 92 earthquakes from all five areas were collected and compiled in order to determine regional trends in principal stresses and thus help estimate the cause for seismicity in each area.

There are five likely causes of seismicity that were considered while examining the principal stresses:

1) Dextral movement along the CCFZ or movement along the Oak Bay fault;
2) Normal faulting related to subsidence due to deposition of sediment within the Bay of Fundy;
3) On-going rifting in the St. Lawrence along Iapetus Rift structures;
4) Vertical movement caused by differential isostatic rebound;
5) Stresses consistent with the passive Atlantic margin.

1.3 Definitions of seismotectonic terms

Before the methods are outlined, it is important to provide brief definitions pertaining to earthquake magnitudes and focal mechanisms. There are several ways to define the magnitude of an earthquake as a function of the availability of data. After USGS, 2009 definitions:

Ms: This type of magnitude is measured on the Richter scale. Ms is defined by the Richter formula: Es= 4.8+ 1.5Ms, where Es is seismic energy in joules.

Me: The energy magnitude is a measure of the shaking from an earthquake measured from higher frequency than Mw. Me is defined by the formula: Me= (2/3) log Es-2.9.

Mo: The seismic moment can be used if Me is not available. Mo is obtained by either measuring the radiated energy from an earthquake (in joules or in dyne*cm) or by calculating from Mw

Mw: The moment magnitude is derived from low-frequency displacement spectra and is a measure of average slip across a fault and area or rupture. It can be obtained by the formula Mw=(log Mo)/1.5-10.7. Mw is then used in the Richter formula to estimate energy radiated from an earthquake.

Mn: the regional or local magnitude is a value used for only North America, east of the Rocky Mountains. It is calculated from short-period surface waves (USGS, 2010).

The magnitudes in this study are reported in Mw, Mn, and Mo. Mw and Mn values are given in GSC open files and in the Global Centroid Moment Tensor database and are used to calculate Mo, as a way to quantify the amount of energy released by earthquakes. For consistency all of the Mo are reported in in dyne*cm and range from 1.99526E+18 dyne*cm to 7.3E+26 dyne*cm with the upper value from the Mn=7.2 Grand Banks earthquake of 1929 (Bent, 1995).

To put into perspective the energy released by earthquakes, see Table 1 for a comparison to TNT and Nuclear energy.

Magnitude	Es (from Me)	Es (from Ms or Mw)	Tons of TNT	Nuclear Bomb Equivalence (# of bombs)
4	0.22E+11	6.3e+17	15.0	0.00
5	0.71E+12	2.0e+19	475.0	0.02
6	0.22E+14	6.3e+20	15023.0	0.79
7	0.71E+15	2.0e+22	475063.0	25.0
8	0.22E+17	6.3e+23	15022833.0	790.6
9	0.71E+18	2.0e+25	475063712.0	25,003.3

Table 1: Comparison of energy released by different magnitudes to the energy released by tons of TNT and nuclear bombs. Es is measured in dyne*cm (after USGS, 2009).

Focal Mechanism: Focal mechanisms can also be referred to as fault plane solutions. They are a means of determining the principal stresses involved in an earthquake and aid in determining the earthquake's cause. A focal mechanism is a depiction of the direction of slip and the orientation of the fault on which it occurs (U.S. Geological Survey, 2010). Focal mechanisms are calculated from the information given by data from many seismograms and plotted onto a stereographic projection (Figures 1.10 and 1.11) a.k.a. "beach ball" diagram.

Two orthogonal planes define a focal mechanism; together they are called nodal planes. One plane represents the actual slip plane i.e., the fault while the other, the auxiliary plane, is complementary to the fault plane. With only a focal mechanism, it is impossible to determine which of the nodal planes the actual fault slip plane is. The nodal planes are constructed by plotting P- and S- wave arrivals from an earthquake to a number of seismic stations (Fossen,

2010). These arrivals are plotted as axes separated by the nodal planes on a focal mechanism diagram, with the P- axis as the compression axis and the T axis as the tension. Different orientations of the P- and T-axes are representative of different fault plane solutions and therefore, different types of faults (Fig. 1.10). The P- and T- axes are not the same as principal stresses, σ_1 and σ_3, but, σ_1 must lie within the P-field and σ_3 in the T-field (Fossen, 2010). σ_1 is on average at 30 ° to the fault plane while the P and T axes are the symmetry axes to the nodal planes and thus are always at a 45° angle to either of them. If there are many observations of earthquakes on variously oriented faults then the approximation of σ_1 and σ_3 are more likely to be accurate (Fossen, 2010).

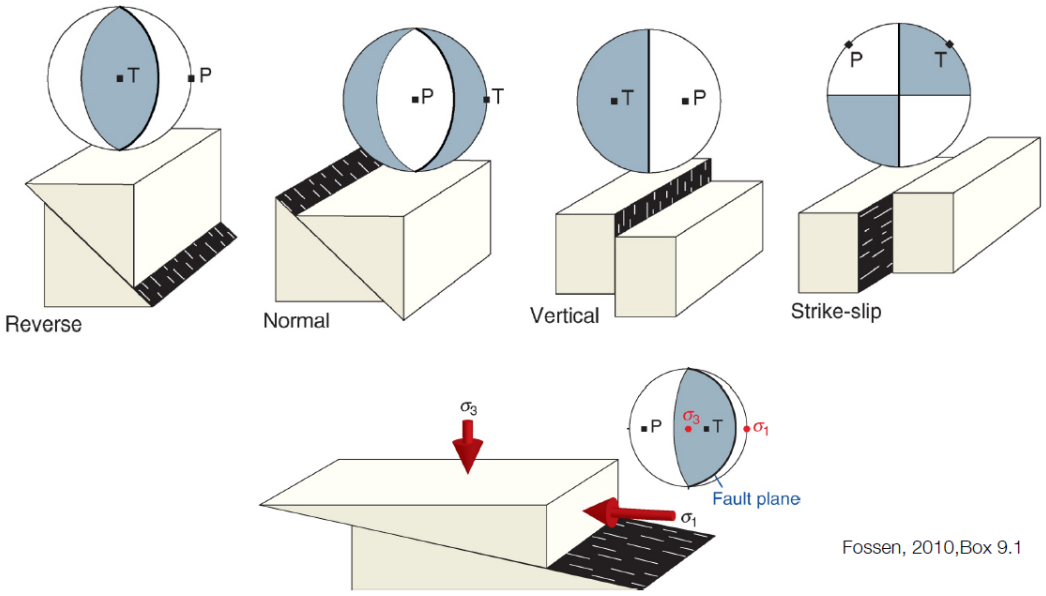

Figure 1.10: Schematic diagrams of typical focal mechanisms showing the type of fault that produces each focal mechanism. T- fields are in grey and P- fields are white (Fossen, 2010).

Another important distinction to make here is that σ_1 and σ_3 are also not the same as σ_H, and σ_h, the horizontal stresses. Anderson's classification of tectonic stress is based on the

orientations of σ_1, σ_2 and σ_3 as three different regimes where at the surface one stress is always vertical σ_v, and the other two are horizontal: where $\sigma_v = \sigma_1$; normal faulting occurs, where $\sigma_v = \sigma_2$; strike-slip faulting occurs, and where $\sigma_v = \sigma_3$; thrust faulting occurs (Fig. 1.11) (Fossen, 2010). The horizontal stresses, σ_H, and σ_h, therefore are the two horizontal stresses in Anderson's classification and can be σ_1, σ_2 or σ_3.

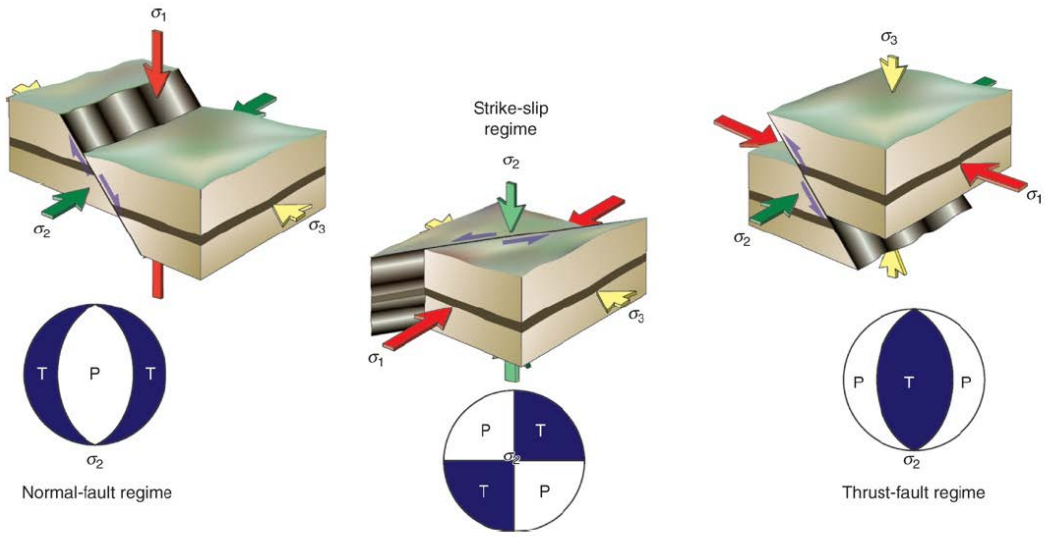

Fossen, 2010, Fig. 5.12

Figure 1.11: Relationship between principal stresses and Anderson's tectonic regimes where stereographic projections show P- and T- axes according to regime. From Fossen (2010).

Focal mechanisms will be used in this study to determine the seismic strain and the regional stress field within the study area. The solutions indicate the sense of tectonic motion in an area, which can be subsequently be attributed to the known regional faults.

1.3.1 Description of Focal Mechanism Data

There are several parameters of reported seismic events that are useful in this study (Fig. 1.12):

Event name: usually named after the date of the event; e.g. 010982A (Fig. 1.12a) happened in 1982 on January 9th (MMDDYY).

Lat: Latitude, where negative numbers are south and positive numbers are north.

Lon: Longitude, where negative numbers are west and positive numbers are east.

Depth: Depth of the earthquake's epicentre below surface in kilometres.

Scalar moment is Mo, see 1.3. See also 1.3 for definitions of Mw and Ms.

Fault planes: Each fault plane is defined by three parameters:

Strike: orientation (angle from 0°-360°) of the line that represents the intersection of the fault on a horizontal plane.

Dip: dip is measured in a vertical plane through a line and the angle is measured from the horizontal plane to the given direction.

Slip: Slip direction of the hanging wall relative to the footwall.

(a) 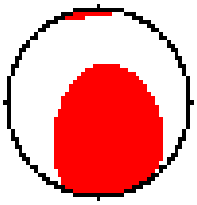 (b) 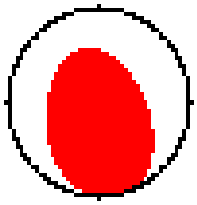

Figure 1.12: Example data from the Global Centroid Moment Tensor Catalog. Two seismic events in the northwest of the study area:

(a) Event name: 010982A NEW BRUNSWICK. Date: 1982/ 1/ 9 Centroid Time: 12:53:53.1 GMT Lat= 46.87 Lon= -66.41 Depth= 10.0 Half duration= 2.5 Centroid time minus hypocentre time: 1.3 Moment Tensor: Expo=24 1.324 0.342 -1.666 -1.107 -0.495 0.296 Mw = 5.5 mb = 5.7 Ms = 4.8 Scalar Moment = 1.94e+24 Fault plane: strike=324 dip=47 slip=42 Fault plane: strike=202 dip=61 slip=129.

(b) Event name: 011182B NEW BRUNSWICK. Date: 1982/ 1/11 Centroid Time: 21:41:11.0 GMT Lat= 47.24 Lon= -66.44 Depth= 15.0 Half duration= 1.4 Centroid time minus hypocentre time: 3.1 Moment Tensor: Expo=23 3.493 0.052 -3.545 -1.651 0.293 0.624 Mw = 5.0 mb = 5.4 Ms = 4.5 Scalar Moment = 3.93e+23 Fault plane: strike=190 dip=44 slip=121 Fault plane: strike=329 dip=53 slip=63

2.0 Methods

2.1 Basis for determining seismic risk

LeBlanc & Kliemkiewicz (1994) define seismic risk as “the probability of occurrence of some adverse consequences of being subjected to a particular hazard”, where hazard is defined as “the potential of occurrence of an adverse event, such as extreme ground shaking from an earthquake, high winds from a storm, flooding from excessive rainfall.”

For the purposes of this study, seismic hazard will be based mostly on proximity of earthquakes to Point Lepreau, orientation of principal stresses with respect to faults near Point Lepreau, frequency of earthquakes, and potential for damage which includes potential of an earthquake in the area to cause tsunamis. Potential for tsunamis is especially important for Offshore Nova Scotia, Laurentian Slope and Grand Banks areas as earthquakes on slopes can lead to submarine slumps which can lead to tsunamis (Bent, 1995).

2.2 Data Compilation

Seismic and structural data were compiled from several sources. Three focal mechanisms were obtained from the Global Centroid Moment Tensor Solution database, ten were obtained from GSC Open File 2430 (Adams, 1991), 13 were obtained from GSC Open File 1892 (Adams et al., 1988), nine were obtained from GSC Open File 1995 (Adams et al., 1989), two from GSC Open file 3870 (Bent & Drysdale, 2000), two from GSC Open File 3698 (Bent & Perry, 1999), one from GSC Open File 4088 (Bent & Perry, 2001), and one from GSC Open File 4289 (Bent & Drysdale, 2002). Included in the study are also focal mechanisms from the 1929 Laurentian Slope Mw=7.2 (Bent, 1995) earthquake and 1975 Laurentian Slope Mw= 5.2 earthquake (Bent, 1995 and Hasegawa & Herrmann,1989). A table of data used for this study may be found in Appendix I.

2.2.1 GSC Open Files

GSC Open files provided data for an average of first motions from many different seismographs, this average is called a "best solution" (Fig. 2.1c). Best solution nodal planes were used to create focal mechanisms (Fig. 2.1) using stereographic plotting software Stereonet (version 7.2.3). After stereograms were made to project the nodal planes for an earthquake, the T fields were coloured grey to differentiate from the fields. All P and T fields for each of the five areas were plotted on separate projections to determine the principal stress regime for each of the five areas.

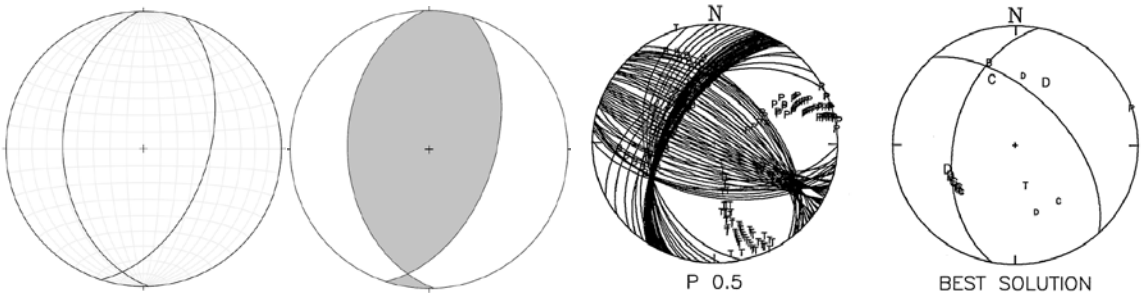

(a) (b) (c)

Figure 2.1: (a) Example of a stereographic projection made in Stereonet, (b) with T field in grey; each of the great circles on the projection is a nodal plane, one is the fault plane and one is the auxiliary plane. (c) Example of first motions from several stations and their best solution (Adams et al., 1988).

2.3 Analytical Methods

2.3.1 Regional stress pattern and World Stress Map data

The 2008 World Stress Map (WSM) is a compilation of the current state of tectonic stress of the Earth's Crust. Tectonic stress (Fig. 2.2) is defined as the local stress state that differs from the reference state of stress due to the influence of a tectonic process where the lithostatic reference state of stress can be described as a state where the vertical and horizontal stresses are equal. This reference state is based on the concept of zero shear stress (σ_s=0), meaning that stress is

completely controlled by the height and density of the overlying rock column: $\sigma_1 = \sigma_2 = \sigma_3 = \rho gz$, where ρ is density, g is the acceleration due to gravity and z is depth (Fossen, 2010). WSM data consist of focal mechanisms, well bore breakout orientations, hydraulic fracturing measurement, overcoring or other strain relief measurement, geologic fault-slip data, geologic-volcanic vent alignment, petal centerline fracture (orientation from mean direction of petal fractures in oriented core), drilling-induced fractures of the borehole wall, and borehole slotter (Heidbach et al., 2009). For the study area, WSM data types included only focal mechanisms (in which case the tectonic regime is known) and well bore breakout orientations (where the regime is unknown). Well bore breakout orientations are measured using the ellipticity of the hole as it indicates the local orientation of horizontal stress axes in the borehole (Fossen, 2010). The WSM data, therefore, are measured using σ_H and σ_h, the maximum and minimum horizontal stresses, respectively.

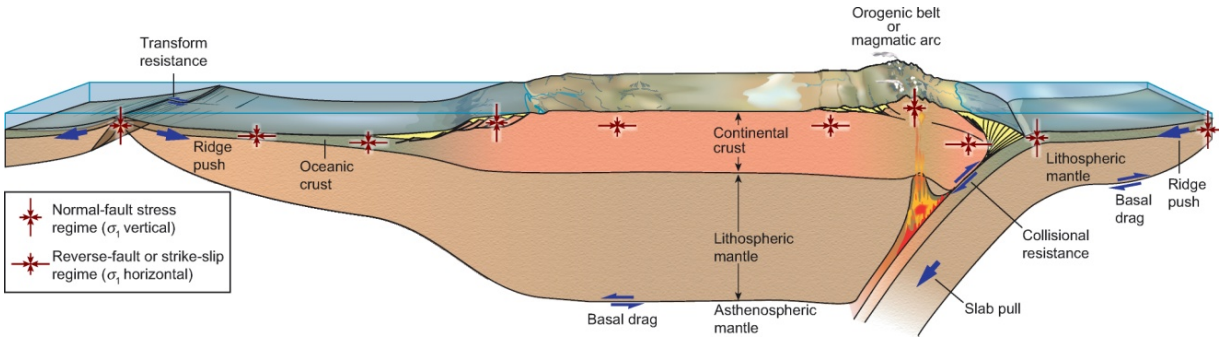

Figure 2.2: Tectonic state of stress showing forces related to tectonics with blue arrows and the corresponding expected stress regimes (red arrows). In continental plates, the maximum stress axis is expected to be horizontal as most plate motion is horizontal except at plate margins. After Fossen (2010).

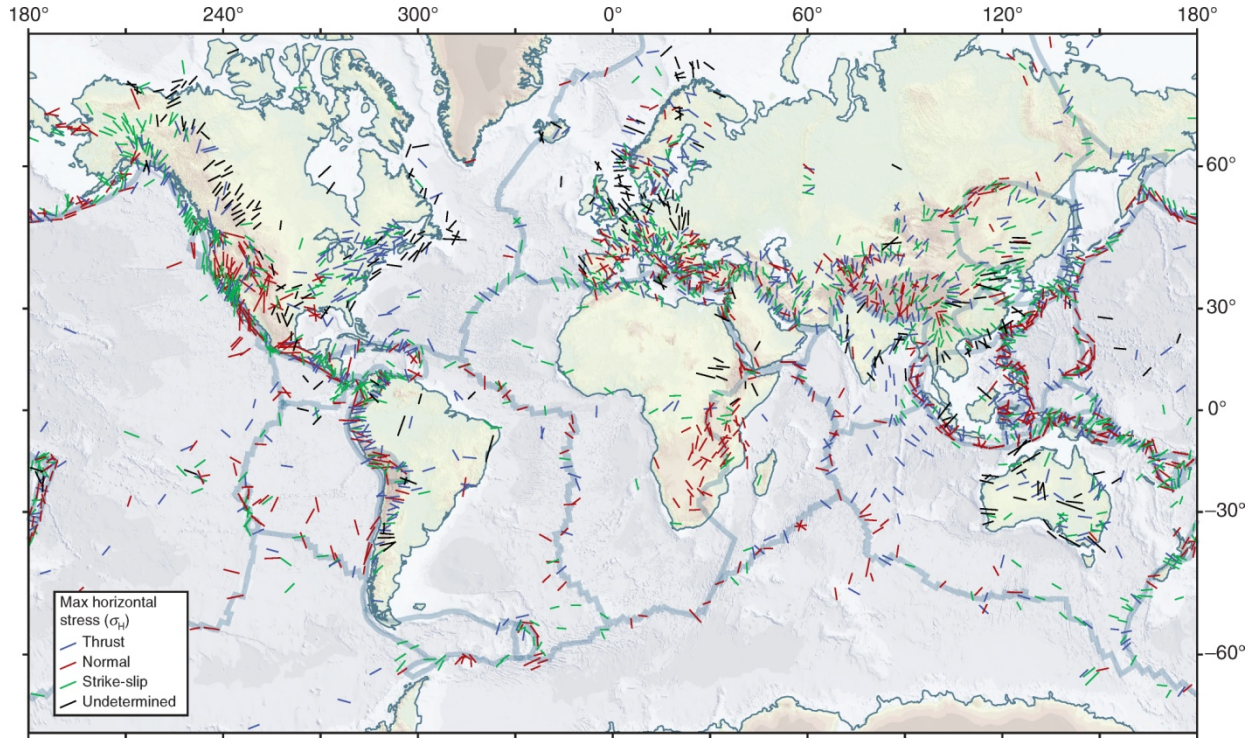

Figure 2.3: Global stress map: Lines represent orientations of maximum horizontal stress σ_H. The tectonic regime is indicated in the inset. After Heidbach et al. (2008).

WSM data were downloaded as a .kmz file from the WSM project's website (http://dc-app3-14.gfz-potsdam.de/pub/stress_data/stress_data_frame.html), mapped in Google Earth Pro and used in conjunction with focal mechanisms to determine regional stress trends. WSM data proved particularly helpful in distinguishing regional stress trends from large-scale trends due to the motion of the North American plate with respect Atlantic ocean; this motion in North America produces a trend (Fig. 2.3).

2.4 GPS Velocity Data

Horizontal velocity data (Craymer et al., 2011) were included in the study to analyse the motion of the North Atlantic plate with respect to the northern portions of the US including Alaska, Greenland as well as a set of global sites and to analyse for local differences in horizontal GPS

motion that could indicate active faults and therefore potential sources of seismicity. Horizontal GPS data differs from the stress data as current plate movement is tracked via satellite and repeated measurements of points on the surface of the Earth are recorded over time to find out the precise location of a plate (or GPS station on the plate) at different time intervals (IRIS, 2012). The velocity of the plate is measured using the distance it has moved in a certain time period. The tectonic stress is resultant from this relative motion and there is a close relationship between the two (Fig. 2.4).

Vertical GPS data were included in the study to analyse vertical motion over Eastern Canada and on a more local scale to observe differences in this motion that could cause fault reactivation. Vertical plate motion usually happens at plate boundaries due to subsidence and orogenic events; one cause of intraplate vertical motion could be isostatic rebound following continental glaciation.

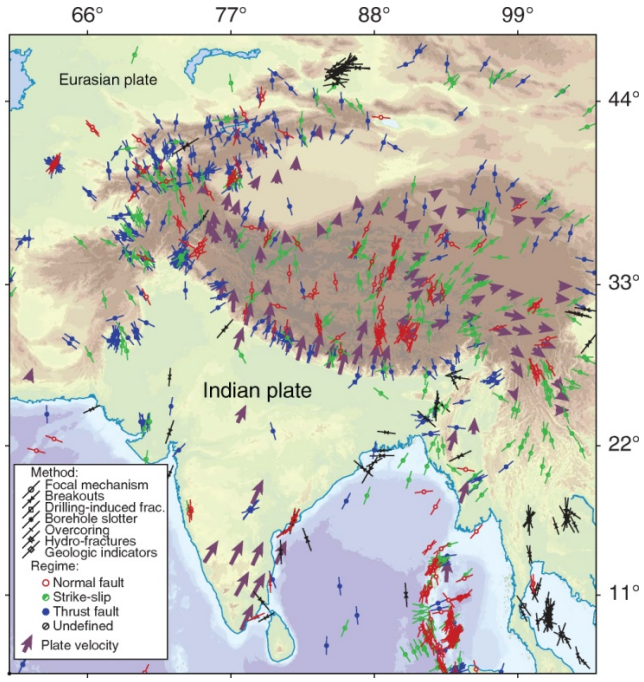

Figure 2.4: Indian and Eurasian plates with GPS velocity data (purple arrows) and WSM stress data (red, green, blue, and black lines). After Fossen, 2010.

3.0 Results

3.1 Crustal state of stress

The World Stress Map (WSM) is a compilation of stress measurements around the world (Heidbach et al., 2008). Compared to tectonically active areas of the world, data in the study area are scarce but in areas with larger recent earthquakes, information on σ_H and the tectonic regime are available.

In the St. Lawrence Gulf, stress measurements (Fig. 3.1) indicate thrust and strike-slip tectonic regime. There are sixteen stress measurements with a known regime for the St. Lawrence Gulf region, fourteen of which are within the St. Lawrence Gulf, one is about 200 km north of Quebec City and another within Chaleur bay, just south of Anticosti Island (Fig. 3.1). Thirteen of the measurements were thrust fault, including the measurement to the north of Quebec City and three were strike slip. Two of the strike-slip measurements are within the Gulf; one near the mouth and one closer to Quebec City while the third strike-slip measurement is in Chaleur Bay (Fig. 3.1).

Laurentian Slope stress measurements are plentiful but based on borehole breakouts, where the ellipticity of the hole gives the orientation of σ_H and σ_h (Fossen, 2010), and there are no stress data with a known regime. The O_H trend at about 20° to 30° (Fig. 3.2). The maximum horizontal stress (O_H) is sub parallel to the motion of the North American plate relative to the Atlantic passive margin.

In the Grand Banks region similarly derived O_H are randomly oriented.

In the Northern Appalachian area there are only three stress measurements, one thrust fault and two strike-slip. On a regional scale, smoothed WSM data show O_H trend of ~20° to 30° throughout most of Eastern Canada (from Quebec to Offshore Nova Scotia) which agrees with the local trends at the Laurentian Slope, in most of the St. Lawrence Gulf and in the Northern Appalachian area (Fig. 3.1, Fig. 3.2).

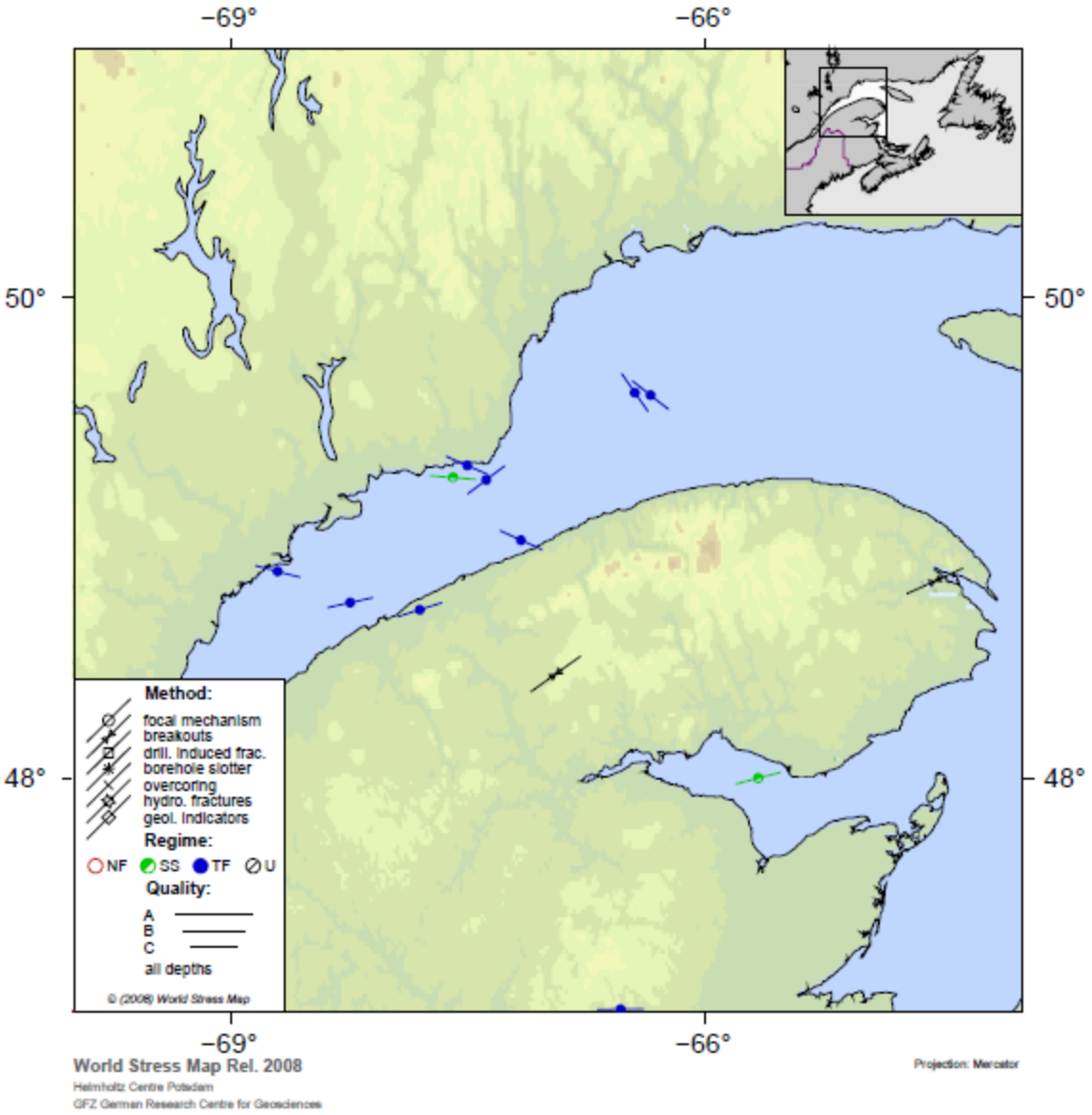

Figure 3.1: WSM data in the St. Lawrence Gulf. Inset shows study area. (After Heidbach et al., 2008)

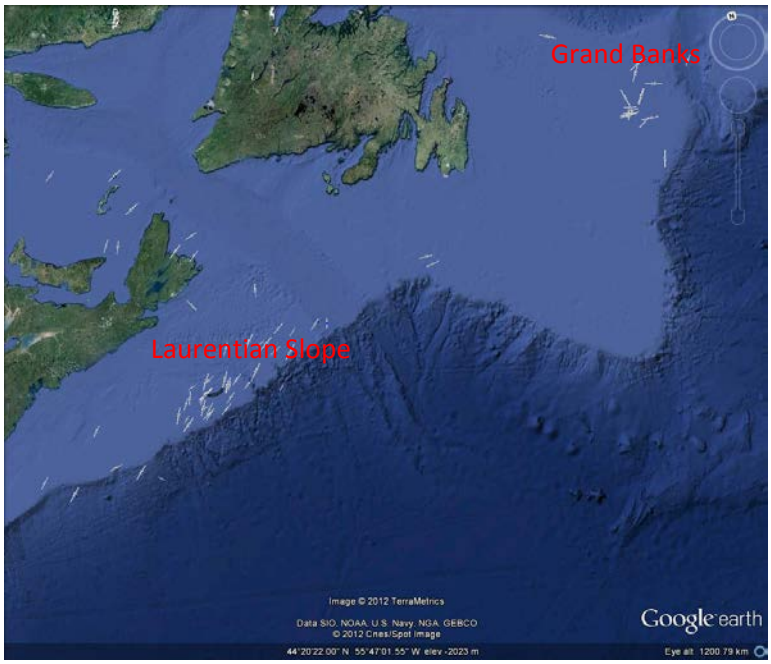

Figure 3.2: Stress measurements in the Atlantic Canada. Laurentian Slope region $\dot{O}_H$ trend ~20° to 30° and are randomly oriented in Grand Banks region. Image taken from Google Earth (2012).

3.2 Focal Mechanism Data

Focal mechanisms were plotted using best solution data from The Geologic Survey of Canada (GSC) studies on earthquakes in Eastern Canada from 1988-2000. The study area is divided in four seismotectonic regions: the Lower St. Lawrence (LSL), Charlevoix (CHV), Northern Appalachians (NAP), and Laurentian Slope.

3.2.1 Lower St. Lawrence

In the Lower St. Lawrence region there are 12 published focal mechanisms (Fig. 3.3); two are strike slip regime and 10 thrust fault. Most of the thrust events have a strike slip component as well. All of the earthquake foci in the LSL region were located between 14 km and 18 km depth.

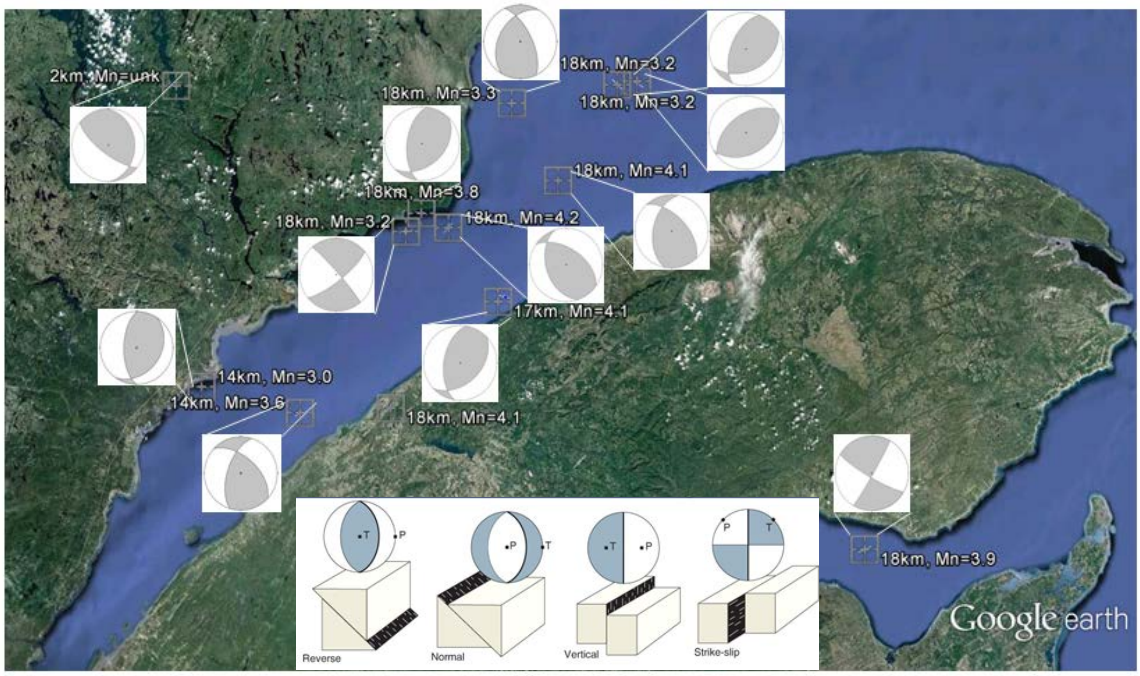

Figure 3.3: Focal mechanisms for the LSL region showing a dominant thrust fault regime and depths focused mostly between 14 and 18 km (topography taken from Google Earth Pro 2012). Inset shows the fault regime that corresponds to each type of focal mechanism (After Fossen, 2010).

3.2.2 Charlevoix

The Charlevoix region had 17 focal mechanisms, three of which were mostly strike-slip regime and 14 thrust regime however, most of the events are oblique slip (Fig. 3.4). The nodal planes on the NE shore (footwall of the rift bounding faults) are mostly NW trending with the exception of two with a NE trend while underneath the river the dominant trend is mostly N-S. There are three clusters of earthquakes in the CHV area (Fig. 3.4): (a) the northwest (b) the northeast shore and (c) the region beneath the river (SW shore). The two shores of the river are separated by the St. Lawrence Fault (Fig. 3.4) The cluster in the northwest is mostly thrust regime with P-fields oriented SW-NE and focal depths between 27.5 km to 29 km. The cluster on the NW shore is mostly thrust regime with P-fields oriented NE-SW and focal depths from 4 km to 20 km. Beneath the river there is another cluster of six focal mechanisms, three of which are thrust regime with no strike-slip component and three are dominantly strike slip with a small component of thrust; P-field orientations here are approximately E-W. Focal depths range

between 10 km and 28 km with four between 10 km and 12 km and two (one in the south and one in the northeast) at 22 km and 28 km, respectively.

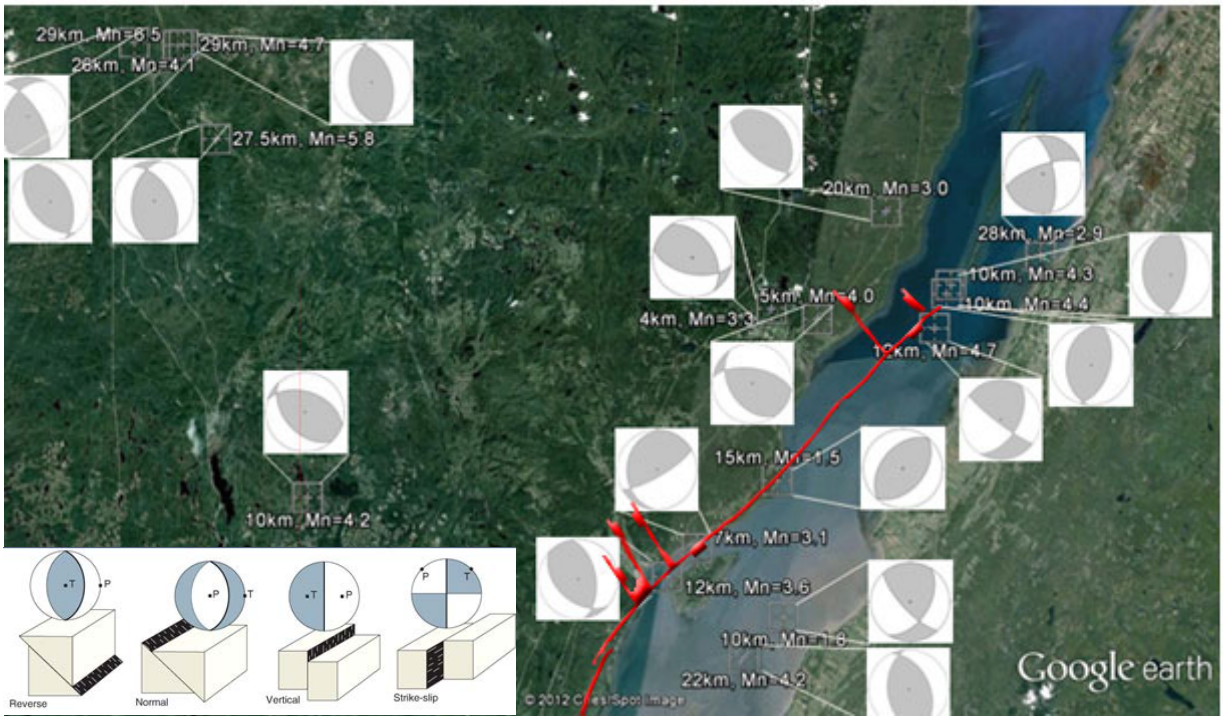

Figure 3.4: Focal mechanisms for the Charlevoix region showing a dominant thrust fault regime (Image taken from Google Earth Pro 2012). Inset shows the fault regime that corresponds to each type of focal mechanism (After Fossen, 2010). Rift faults in the St. Lawrence Gulf (in red) showing fault separation of the two shores of the St. Lawrence by the St. Lawrence Fault (main fault, parallel to St. Lawrence River). Modified from Tremblay & Lemieux (2001).

3.2.3 Northern Appalachians

In the Northern Appalachian region, eight focal mechanisms were determined, showing mostly thrust faulting regime with one strike slip regime (Fig. 3.5). All the thrust faults are somewhat oblique. Focal depths of earthquakes in the NAP region vary from 4 km to 15 km with two focal depth clusters, one from 10 km to 15km and the other 4km to 5km. The earthquakes are spatially clustered but show no focal depth trend.

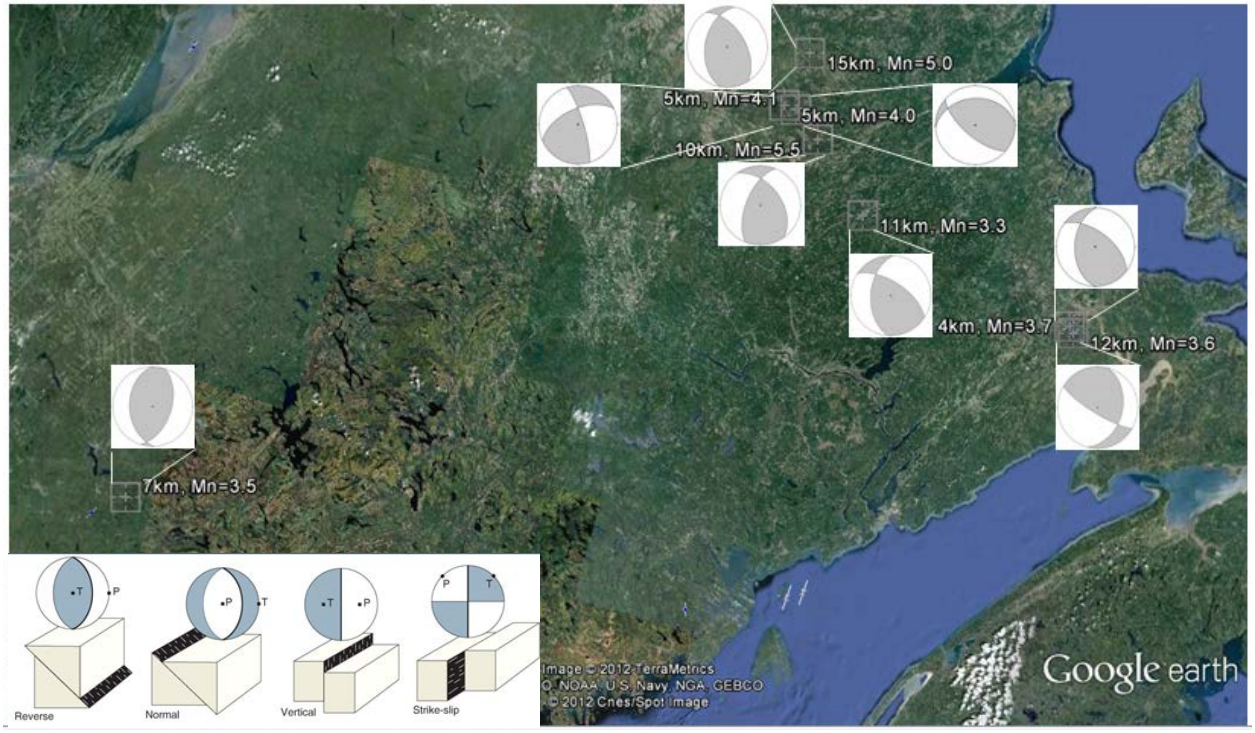

Figure 3.5: Focal mechanisms for the Northern Appalachian region showing a dominant thrust fault regime (Topography taken from Google Earth Pro 2012). Inset shows the fault regime that corresponds to each type of focal mechanism (After Fossen, 2010).

3.2.4 Laurentian Slope

The Laurentian Slope (LSP) area had three focal mechanisms, all located within the Laurentian channel's slope area. One earthquake had a thrust regime while the others were mostly strike-slip with a thrust component. The magnitudes and focal depths of these earthquakes can be seen in Fig. 3.6.

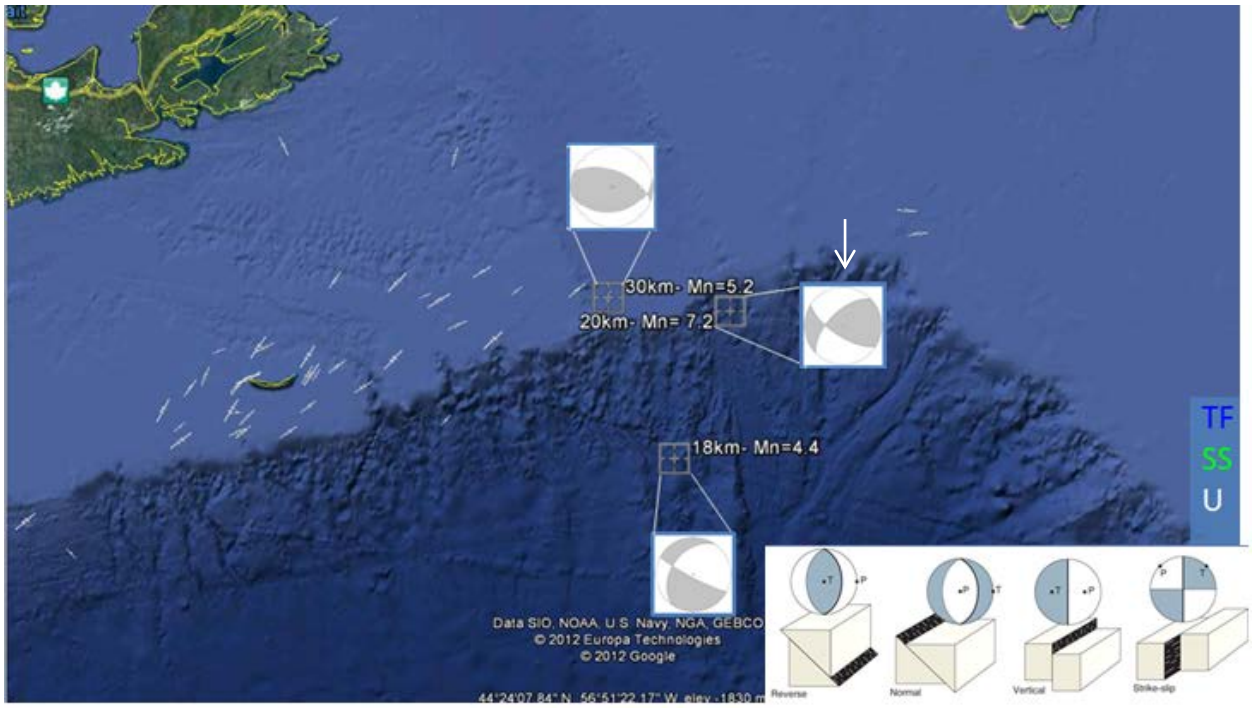

Figure 3.6: Map showing focal mechanisms for three earthquakes on the Laurentian Slope, the Mn=7.2 earthquake of 1929 is indicated with an arrow (Topography taken from Google Earth Pro 2012). Inset shows the fault regime that corresponds to each type of focal mechanism (After Fossen, 2010).

3.3 P and T Axes

P and T axes were compiled and plotted on stereographic projections for each of the four regions to determine the trends for each region (Fig. 3.7). In the Charlevoix and Lower St. Lawrence regions, P-axes are oriented ESE-WNW. The Northern Appalachian region indicate a thrust faulting regime, with the P- axes oriented NNE-SSW and vertical T-axes. The three regions plotted together show an overall thrust regime and the when plotted together in figure 3.7, all P-axes are sub-horizontal and T-axes dip moderately to sub-vertically.

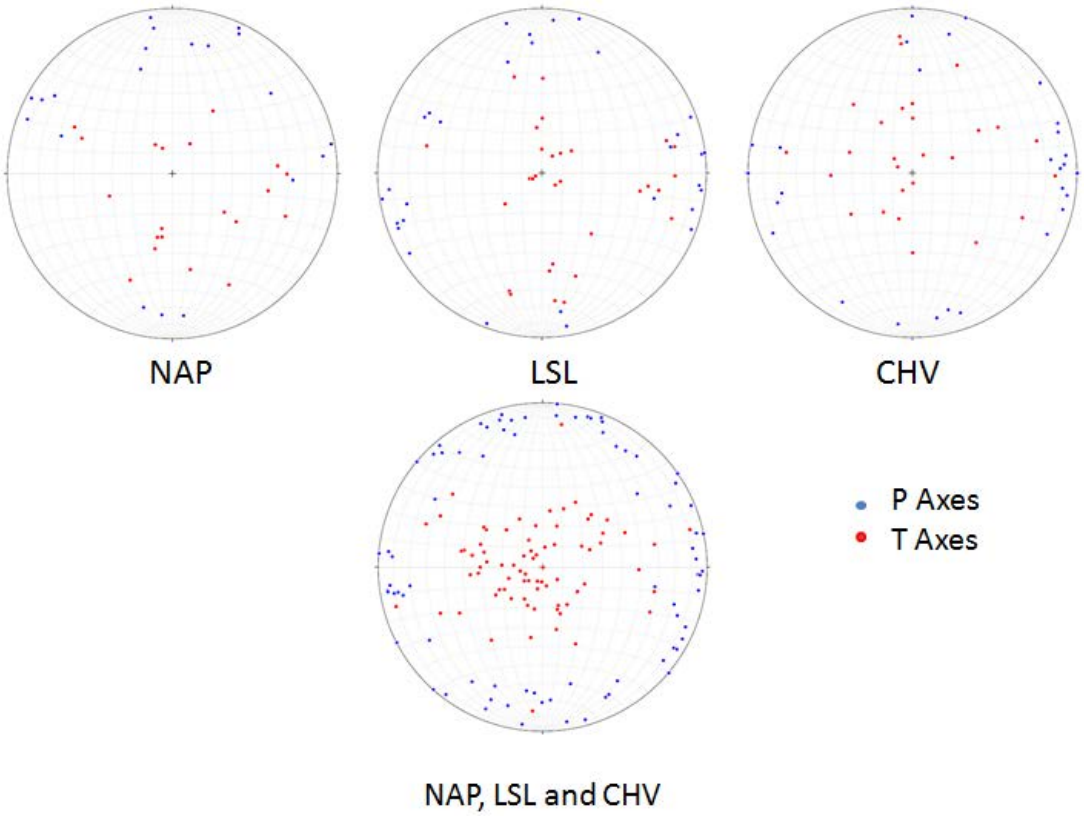

Figure 3.7: P and T axes for Northern Appalachian (NAP), Lower St. Lawrence (LSL) and Charlevoix (CHV) regions. Red points are P axes and blue points are T axes. Diagrams prepared with FaultKin v. 5.2.6.

In the Lower St. Lawrence zone, ten focal mechanisms are thrust regime and two strike slip. Five of the ten thrust events have nodal planes trending NE-SW and the other five thrust regime solutions have nodal planes that trend NW-SE or NNW- SSE. The nodal planes of the two strike slip events in this region are oriented roughly the same way, in a N-S direction. Therefore, on the average solution for LSL, P- axes are oriented ENE-WSW (Fig. 3.7).

The Charlevoix region had focal mechanisms in three different clusters (Fig. 3.4); nodal planes in the NW of the map area in Fig. 3.4 are oriented in a thrust-regime with P-axes trending NE-SW and vertical T-axes. The cluster on the NE shore are all thrust regime and have P-axes trending mostly NE with the exception of two that have a NW trend. Underneath the river the dominant P-axis trend is mostly E-W.

In the NAP region most P-axes trend NE-SW, with the exception of two that trends E-W, one of which is ~300 km west of the other seven events and the other is strike slip regime.

The Laurentian slope area had three focal mechanisms, two strike slip and one thrust fault. The 1929 Mn-7.2 earthquake is the only one for which the actual fault plane is distinguishable from the auxiliary plane (Bent, 1995).The P-axes for the 1929 earthquake and the 1975 earthquake both trend N-S, although the 1975 event is thrust regime (Bent, 1995). The Mn= 4.4 event is further down the slope and its P-axis trends WNW-ESE.

4.0 Discussion

4.1 World Stress Map

All regions showed WSM data that indicated the $\dot{O}_H$ trend is ~20° to 30°. There are some local variations in the CHV, LSL, and NAP regions but the Laurentian Slope region agreed with the data. The Grand Banks region did not agree with the $\dot{O}_H$ trend of ~20° to 30° or show any trend at all. The North American plate's motion is measured by satellites using repeated measurement of points on the surface of North America (IRIS, 2012). The differences in motion seen, for example, in the LSL, CHV and NAP zones are manifested as active faults. $\dot{O}_H$ is almost perpendicular to the motion of the North American plate (Fig. 4.1) and σ_h is approximately 110°-120°, perpendicular to $\dot{O}_H$.

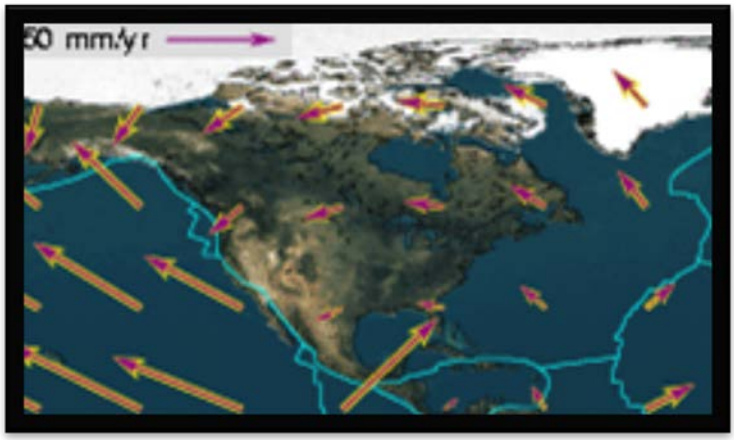

Figure 4.1: Motion of the North American plate is approximately perpendicular to the $\dot{O}_H$ across North America (Fig. 3.2). (IRIS, 2012).

This suggests that on a regional scale, the state of stress is due to the motion of the North American plate while locally at CHV, LSL and NAP where variations are seen, the active Iapetan Rift faults seem to influence the local state of stress.

4.2 Focal Mechanisms

Focal mechanisms show variation locally in all regions. The Charlevoix region shows three clusters of events (Fig. 3.4): (a) the northwest (b) the northeast shore and (c) the region beneath the river (SW shore). The northeast shore and region beneath the river are separated by the St.

Lawrence and Cap-Tourmente faults (Fig. 3.5). The St. Lawrence Fault is parallel to the St. Lawrence River and trends N020°-N050° and dips 60°-70° SE (Tremblay & Lemieux, 2001). The Cap-Tourmente Fault trends east and dips steeply (~80°) to the south (Tremblay & Lemieux, 2001) (Fig. 3.5). The Cap-Tourmente Fault is thought to be a transfer fault to the St. Lawrence Fault and both show cross-cutting relationships. The apatite fission-track ages indicate the fault system was re-activated in the Mesozoic, concurrent with the opening of the Atlantic Ocean (Tremblay & Lemieux, 2001). There is a difference in focal mechanisms between the footwall and hanging wall of the rift faults. The region on the northeast shore (footwall) shows P- axes trending mostly 20° to 30° while the region below the river (hanging wall) shows a P-axis trend that is approximately E-W. T-axes in both cases are mostly vertical except in the case of oblique faults where T-axes are somewhere between vertical and horizontal. The region in the NW of the CHV seismic zone shows focal mechanisms similar to that of the region beneath the river; P-axes trend E-W or ESE-WNW, and T-axes are vertical as all five focal mechanisms are thrust regime. P-axes here are consistent with the σ_H, indicating that the events here could be a result of stress due to motion of the North American plate, accommodated by local faults.

The LSL region contained 12 focal mechanism; ten thrust fault and two strike-slip. Most of the thrust events are oblique. All the earthquake foci in the LSL region are supracrustal, located between 14 km and 18 km depth. In the LSL region the σ_H and P and T sectors (Fig.s 3.2 and 4.2) suggest that the principal stress in the LSL is due to stress from the motion of the North American plate (Fig. 4.1). Iapetan Rift structures continue into the LSL zone (Fig. 4.3) though most events (with the exception of one) are in the hanging wall of the St. Lawrence fault. P-axes in the LSL region are bimodally distributed with five trending NW-SE, five trending SW-NE and two strikeslip. P- and T- axes when plotted together show an average thrust regime solution with mean T- axes sub-vertical and mean P- axes sub-horizontal, trending 20° - 30° N.

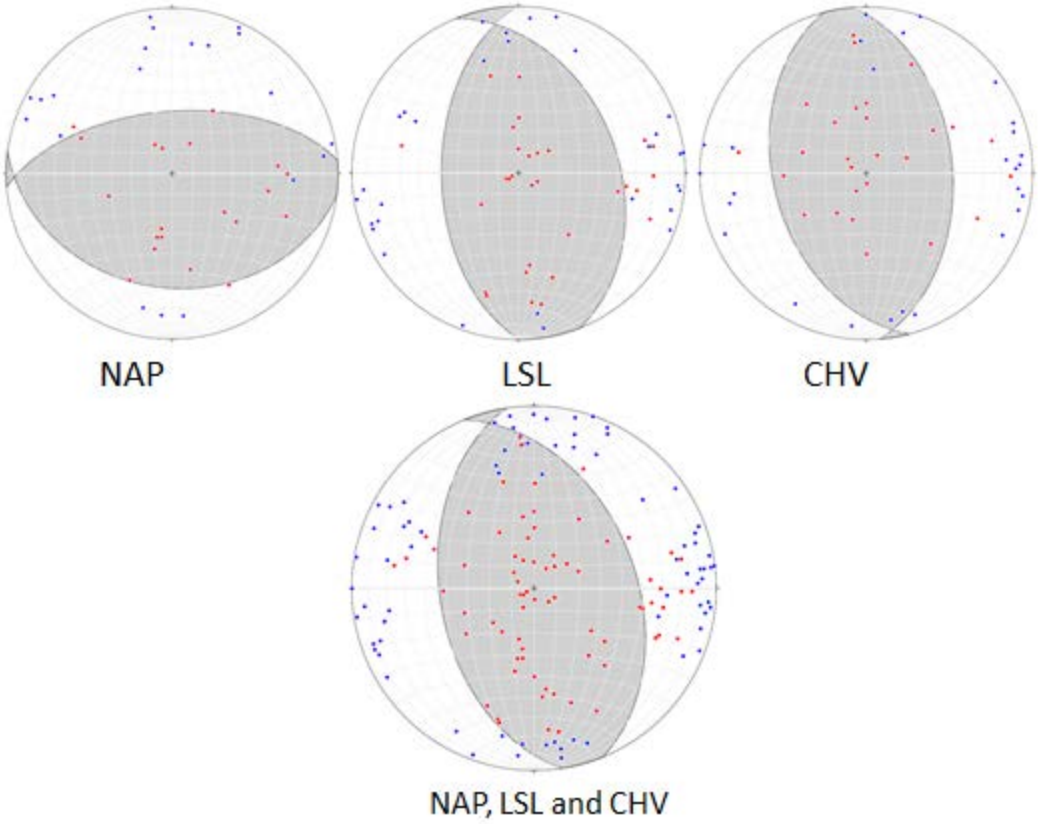

Figure 4.2: P and T axes for NAP, LSL and CHV areas and all three areas together. P-axes are in blue, T-axes in red. Average T- sector is shaded grey and average P- sector in white. (FaultKin v.5.2.6). There is some overlap for this dataset; the P and T axes do not always plot within two sectors that are separated by two mutually orthogonal nodal planes. For this reason, the data seen here may be the result of two different stress fields.

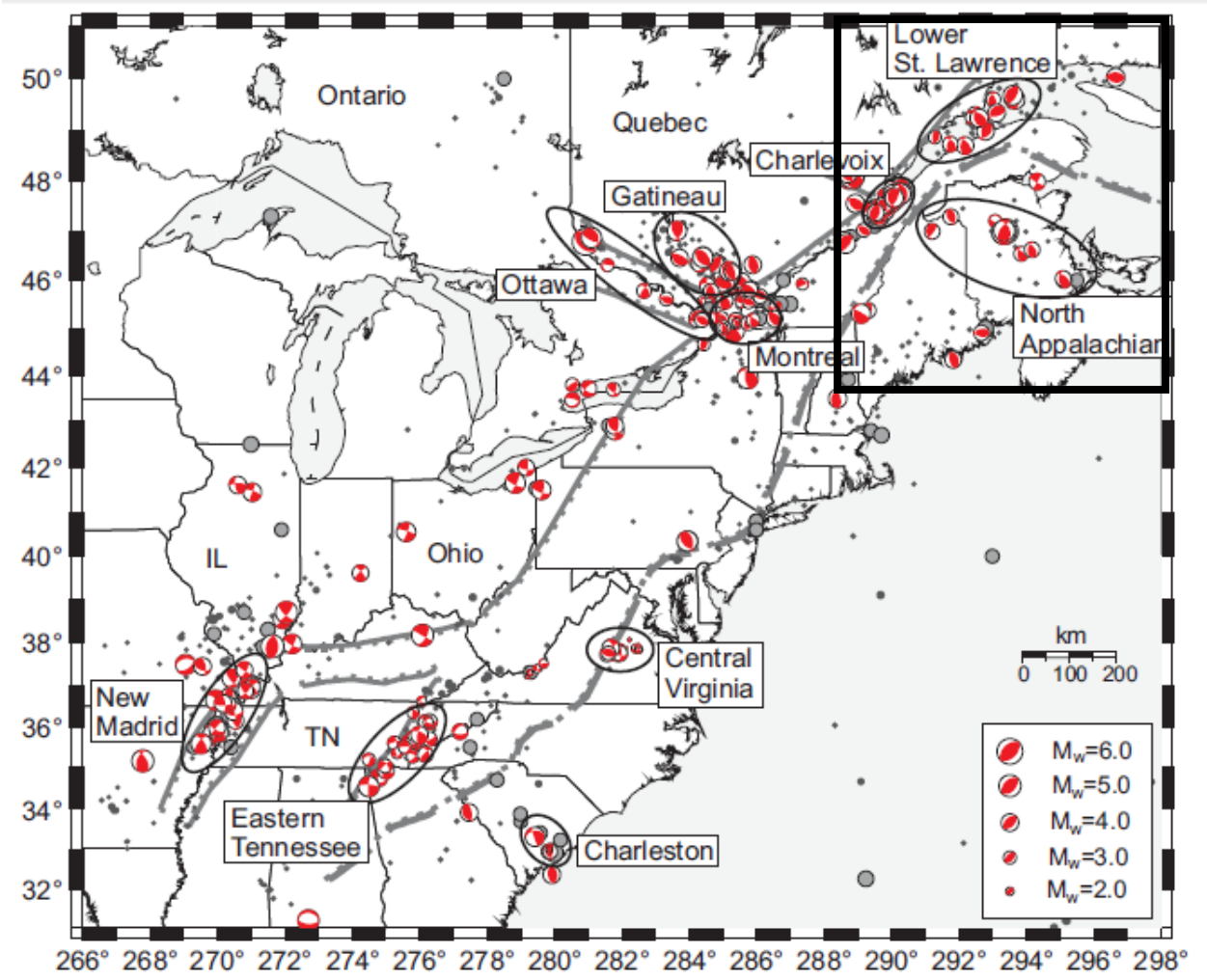

Figure 4.3: Seismic zones and their focal mechanisms of eastern North America. The box indicates the 3 study areas and the Iapetan rift structures (thick, grey lines). (After Mazzotti & Townend, 2010).

The NAP region is bounded on the northwest side by Iapetan Rift faults but is not fault-bounded on the west. The NAP region showed an average thrust regime (Fig. 4.2) like the CHV and LSL regions, but the average focal solution showed a different orientation of P-axes which are oriented NNW-SSE compared to the NE-SW orientation of the LSL and CHV areas. This change in orientation of the P-field is significant; it indicates that the direction of largest principal stress is the in same direction as the LSL and CHV areas from the NAP zone. It is likely a combination of rifting in the NW and compressive stress due to plate motion that produces this average NNW-SSE P-axis trend.

The Laurentian Slope zone had three focal mechanisms; one of which is for the 1929 Mn= 7.2 event (Bent, 1995), one is for the 1975 Mn= 5.2 earthquake (Hasegawa & Herrmann, 1989) and the third is for a Mn= 4.4 event in 1998 (Bent & Perry, 1999). The Laurentian Slope area is significant because it is (a) the source of the largest earthquake in the study area and (b) because it is the only region for which the fault plane is known.

All three earthquakes are between 18 km and 30 km depth. The crust in this area is approximately 25-30 km thick (U.S. Geological Survey, 2009), therefore a shallow crustal source can be ruled out and an uppermost mantle source is possible (Bent, 1995). The 1929 event had a primarily strike-slip regime (Fig. 4.4) and the 1975 event had a solution that was dominantly thrust regime (fault plane unknown) therefore, the possibility of a large thrust event in the LSP region cannot be ruled out (Bent, 1995). There are three subevents to the 1929 earthquake; the first of which ruptured right laterally along a fault that trends approximately parallel to the Newfoundland Fracture Zone (Fig. 4.4), the second and third subevents are offset to the NW but also ruptured right-laterally along faults that trend subparallel to the continental slope (Bent, 1995).

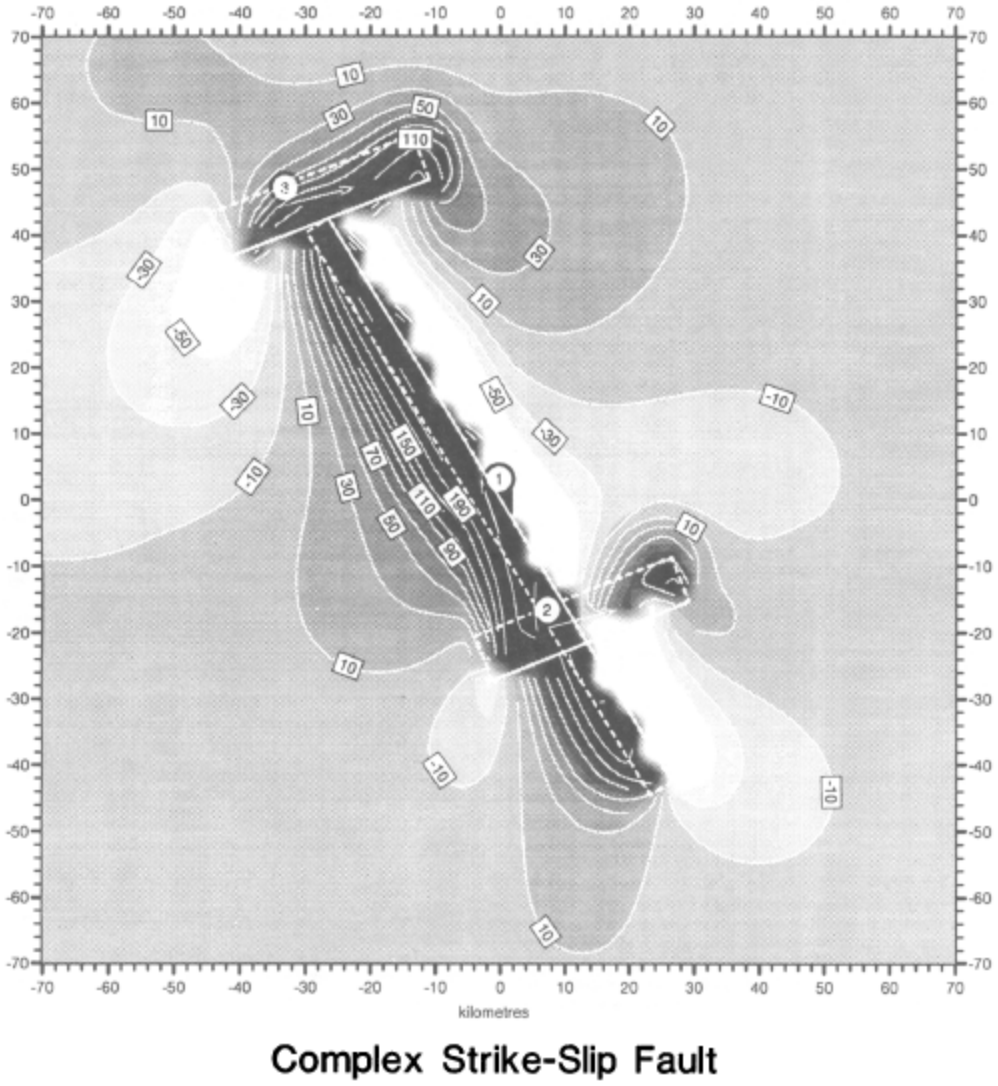

Figure 4.4: Fault plane solution for the 1929 Mn 7.2 event on the Laurentian Slope. Contour labels in boxes show seafloor displacement in millimetres. The main event's epicentre is at the southeast end of fault 1 and horizontal distances are measured from the centre of the largest fault. The subevent number is indicated in a circle and dashed boxes show the surface projection of the faults. (After Bent, 1995).

4.3 GPS Velocities

Horizontal and vertical GPS velocity data are incorporated into the study using data from a NRCAN study (Craymer et al., 2011). Horizontal velocities are defined with reference to the northern portions of the US including Alaska, Greenland as well as a set of global sites and show most of Canada moving to the southwest at a rate of ~20mm/year (Fig. 4.5).

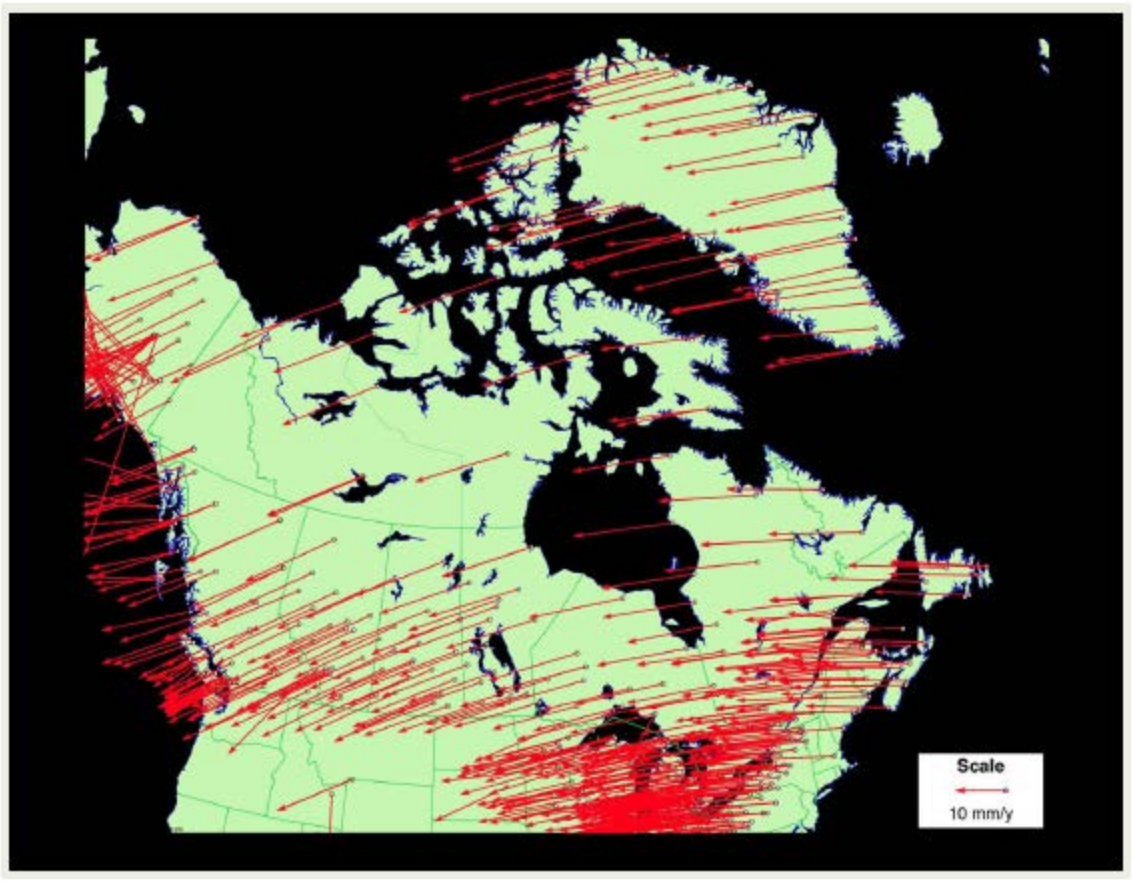

Figure 4.5: Horizontal velocity across North America with respect to the northern portions of the US including Alaska, Greenland and a set of global sites (Craymer et al., 2011).

In the eastern Canada the relative horizontal velocities are insignificant except in the St. Lawrence Gulf where there is differential horizontal motion. The north shore is moving to the southeast at a rate of ~3 mm/yr with respect to Atlantic Canada to the direction of the SE and the south shore is moving to the SE at a rate of ~1 mm/yr (Fig. 4.6). The movement of the south shore can be accounted for by motion of the St. Lawrence fault as the south shore is in the hanging wall of the fault. Nova Scotia and New Brunswick seem to be moving with the North American plate. Movement to the southeast along the north shore (in relation to Atlantic Canada) occurs just past the LSL zone, where the St. Lawrence fault curves into the north shore so, this area is also in the hanging wall of the St. Lawrence fault which explains its movement toward the southeast (Fig. 4.3) (Tremblay & Lemieux, 2001).

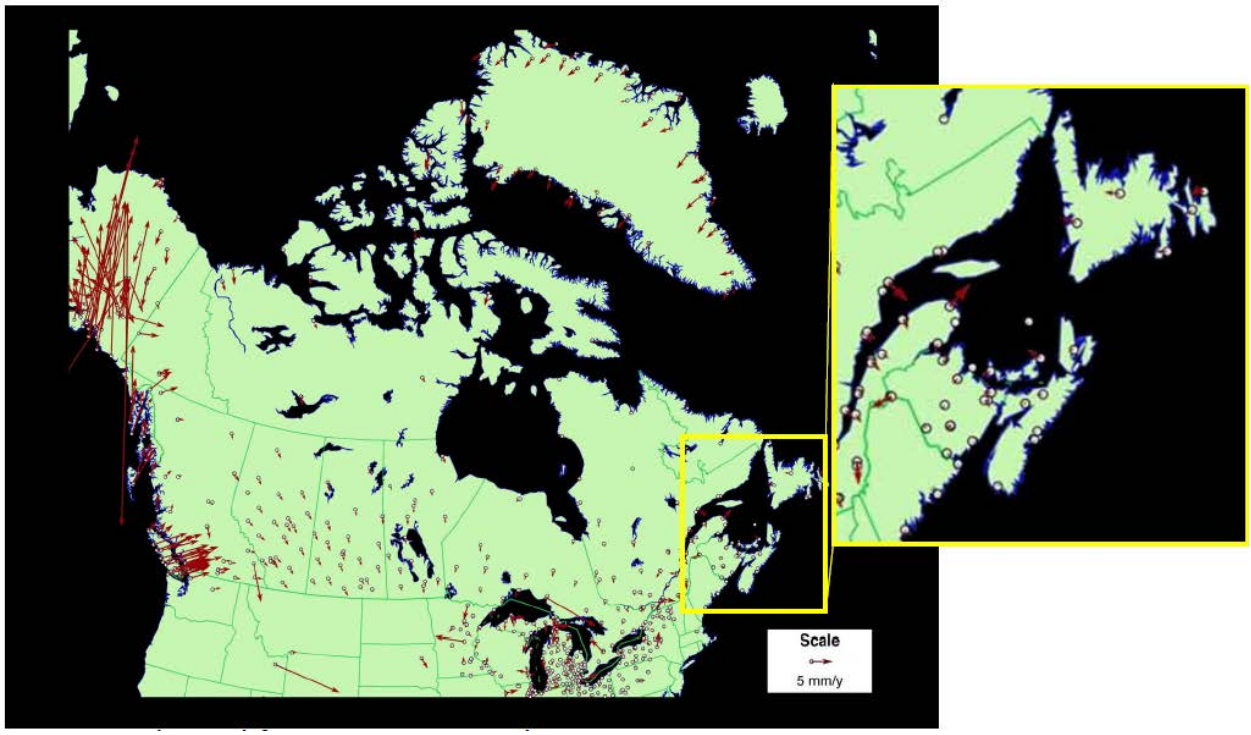

Figure 4.6: Relative horizontal GPS velocities in North America. The Gulf of St. Lawrence shows differential horizontal motion while throughout the rest of Atlantic Canada there is insignificant differential horizontal motion (after Craymer et al., 2011).

Absolute vertical GPS velocities of Canada show uplift over most of the country The CHV and LSL regions are uplifting at approximately the same rate as eastern Canada (Fig. 4.7) and eastern Canada shows ~5 mm/yr uplift in the St. Lawrence Gulf (Fig. 4.7). In the NAP region, there is less uplift and in northern New Brunswick while in Nova Scotia, there is subsidence of up to ~4 mm/yr. This change in vertical motion could cause torque that can reactivate faults between the St. Lawrence Gulf and Nova Scotia.

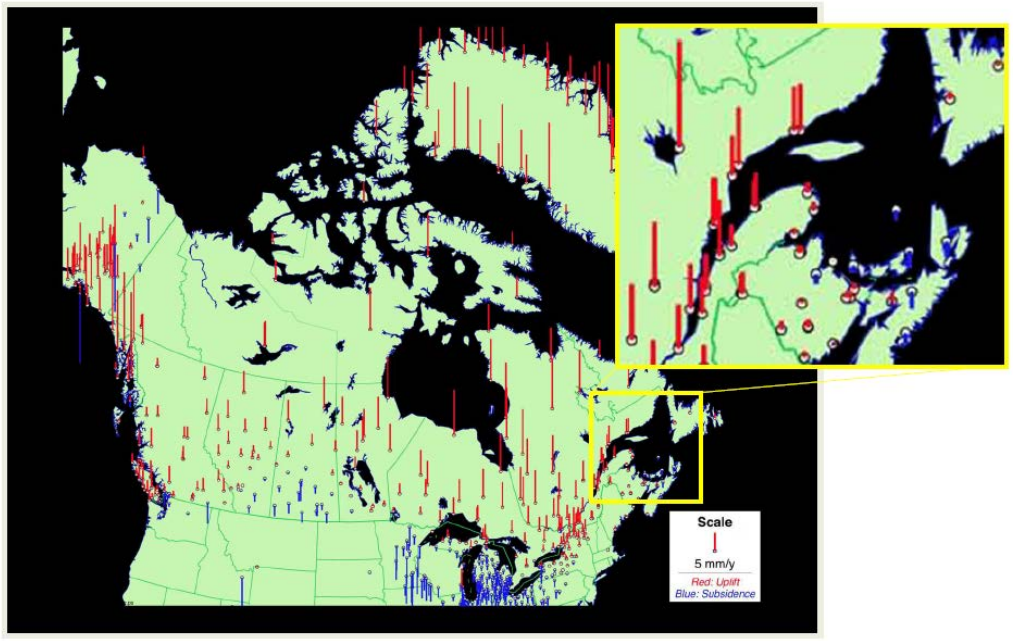

Figure 4.7: Absolute vertical GPS velocities of Canada. Red is uplift, blue is subsidence. Notice differential vertical motion between the St. Lawrence Gulf and Nova Scotia. (After Craymer et al., 2011).

4.4 Slip Inversion

4.4.1 Hanging wall slip data

All the hanging wall slip directions are consistent with the reverse slip regardless of the slip plane orientation (Fig. 4.8). In the Charlevoix region, hanging wall slip plots show clusters of slip directions in the NE-SW (dominant), NW –SE (subordinate). The LSL region also shows a bimodal distribution of hanging wall slip directions, with a cluster in the NE-SW (dominant), and a cluster in the NW –SE (subordinate) (Fig. 4.8).

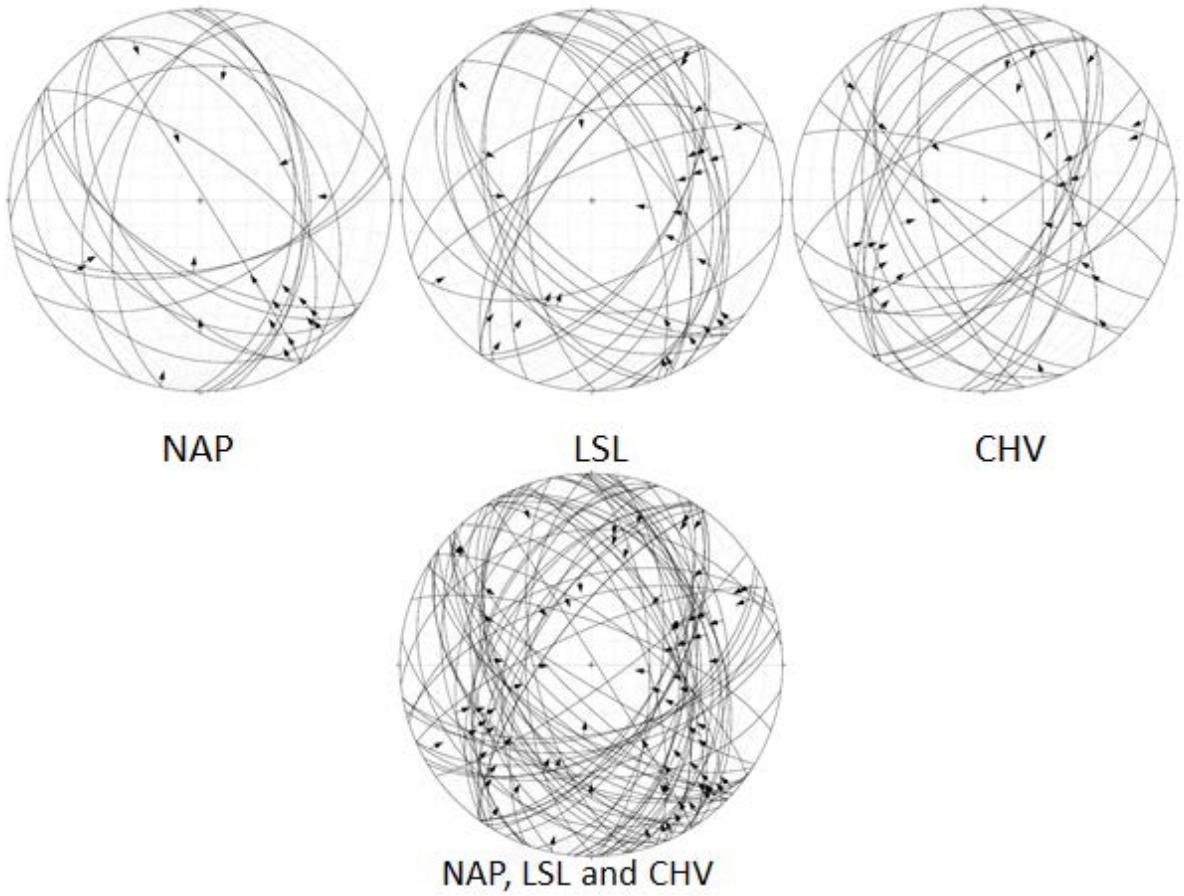

Figure 4.8: Hanging wall slip plots show the motion of the hanging wall of a fault plane with fault planes indicated by great circles and the direction of slip on the hanging wall shown by the arrow. Hanging wall slip directions for Northern Appalachian (NAP), Lower St. Lawrence (LSL) and Charlevoix (CHV) regions. Each nodal plane was treated as a slip plane and the slip directions were determined from the focal solutions. (Created with FaultKin v. 5.2.6)

The hanging wall slip data for the NAP region have one cluster of slip lines dipping to the SE (with hanging wall motion to the NW) and the data for all regions together show that all slip planes indicate reverse motion (Fig. 4.8)

Kinematic axes were found for both the CHV and NAP zones in order to calculate the strain on the St. Lawrence and Oak Bay faults, respectively. Data were insufficient for the LSP, and Grand Banks region.

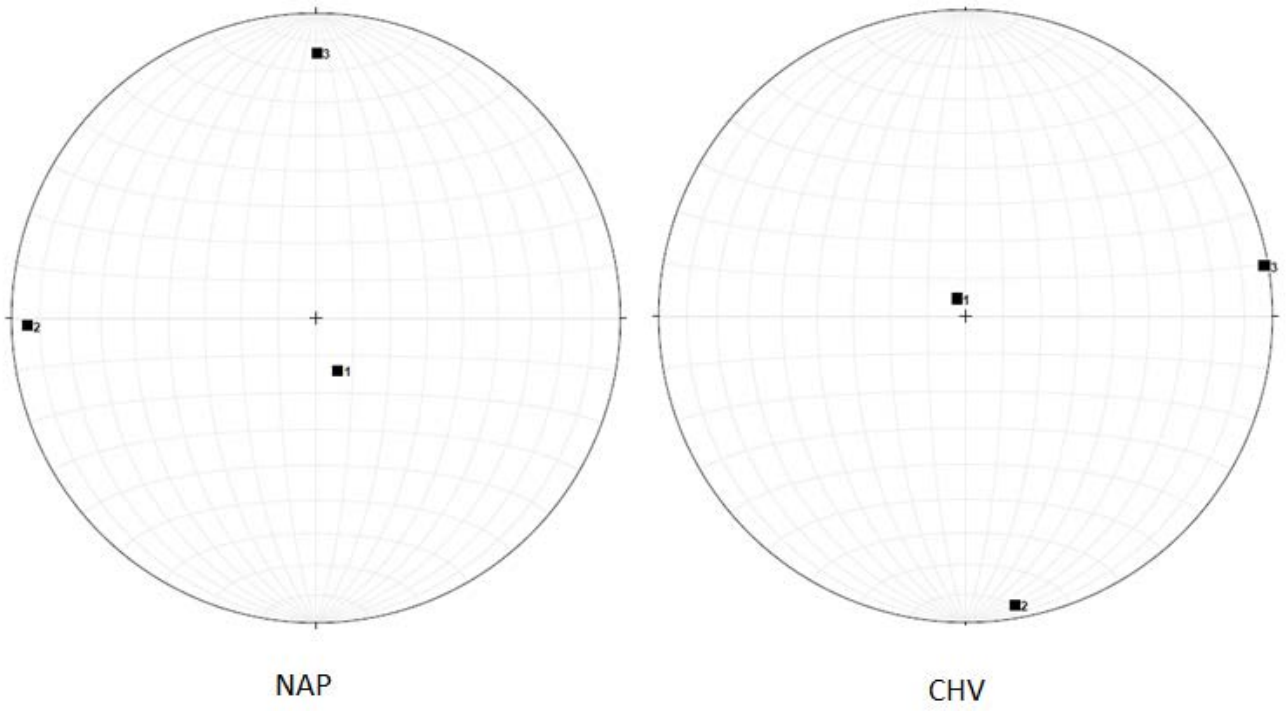

Figure 4.9: Kinematic axes for the NAP and CHV regions found using stress inversion. NAP: 1=σ_3; 2 =σ_1, 3=σ_2 CHV: 1=σ_3; 2 =σ_2 , 3=σ_1.

Kinematic axes both show thrust regime with σ_3 subvertical to vertical and different orientations of σ_1, indicating that the principal compressive stresses for each region are not the same.

4.5 Stress inversion

Paleostress inversion was used to obtain the relative magnitudes of the principal stresses. Stress inversion involves the reconstruction of the orientation and shape of the stress ellipsoid based on the measured fault slip data (Fossen, 2010). Two methods can be applied: Tangent lineation plots show the direction of the tangent to the fault plane lineation. With the assumption that movement is parallel to the direction of maximum shear stress, these plots show patterns that depend on the ratio of shear stress (σ_1 to σ_2), allowing for interpretation of the orientation of principle stresses (Fossen, 2010). The stress ratio: $\phi = (\sigma_2 - \sigma_3)/(\sigma_1 - \sigma_3)$ is used where $0 \leq \phi \leq 1$; $\phi = 0$ for a prolate stress ellipsoid (uniaxial compression), $0 < \phi < 1$ is plane strain, and $\phi = 1$ for an oblate ellipsoid (uniaxial tension).

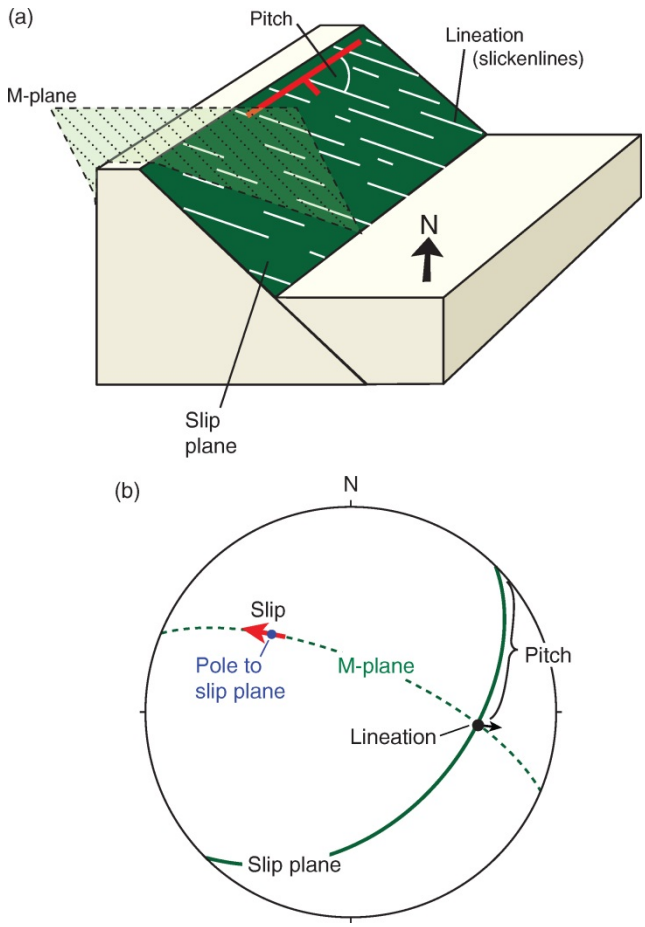

Figure 4.10: Illustration of (a) a pitch measured on the surface of a fault, (b) stereographic projection showing the pitch from (a) and the tangent lineation. The tangent lineation (red arrow) is found by plotting a plane (the M-plane in (a)) that contains the lineation and the pole to the slip plane. The tangent lineation is drawn tangential to the M-plane at the pole to the slip plane and its direction shows the movement of the footwall relative to the hanging wall. This diagram shows normal movement as the footwall moves down toward the west. After Fossen (2010).

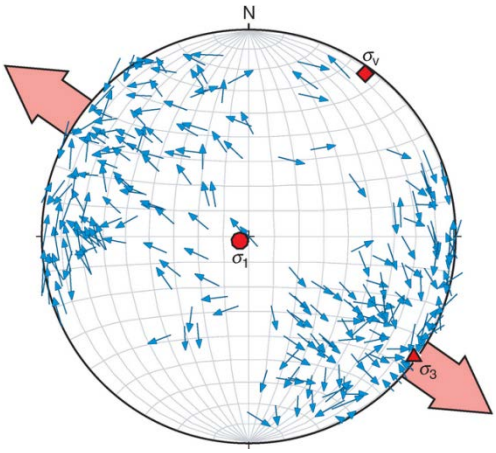

Figure 4.11: Example of Tangent lineation diagram showing a ϕ value of 1, indicating that $\sigma_1 = \sigma_2$ (see Fig. 4.12). Arrows show movement of the footwall. (After Fossen, 2010)

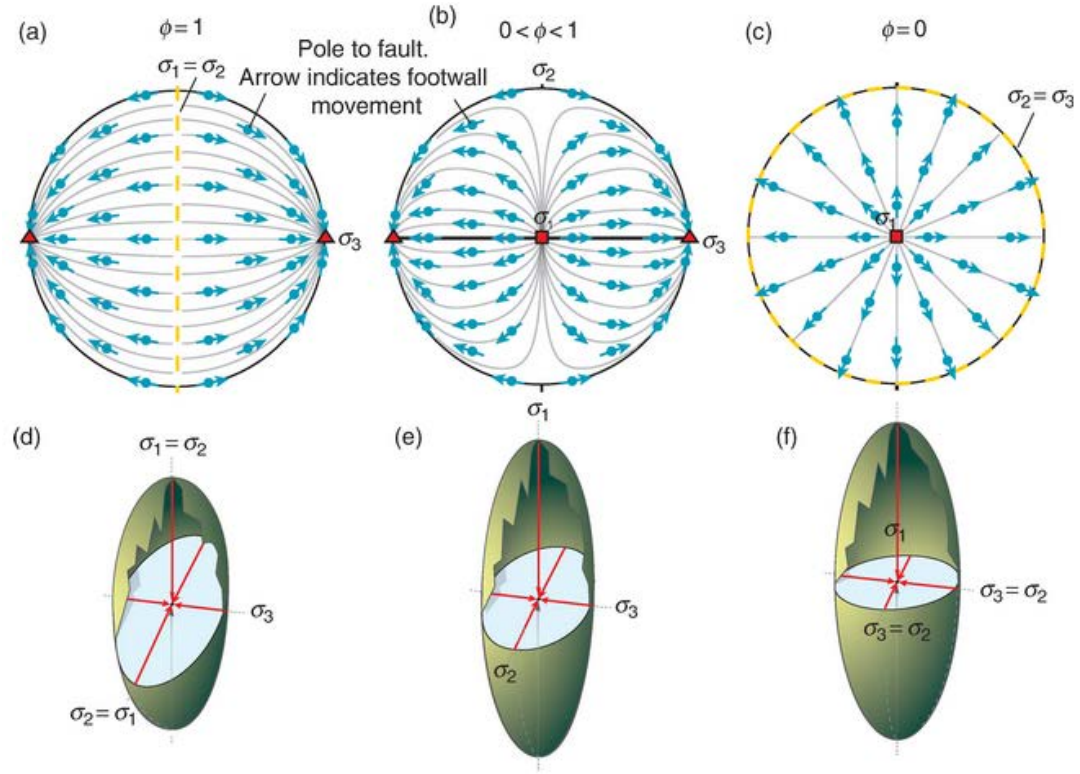

Figure 4.12: (a-c) Stereographic projections; points show poles to faults and arrows show the movement of the footwall. The patterns of footwall movement show the ratio between the principle stresses (ϕ). The corresponding strain ellipsoid is shown for each case (d-f).

Tangent lineation plots for NAP, LSL, and CHV (Fig. 4.8) show a pattern similar to that of Fig. 4.11 and Fig. 4.12 (a).

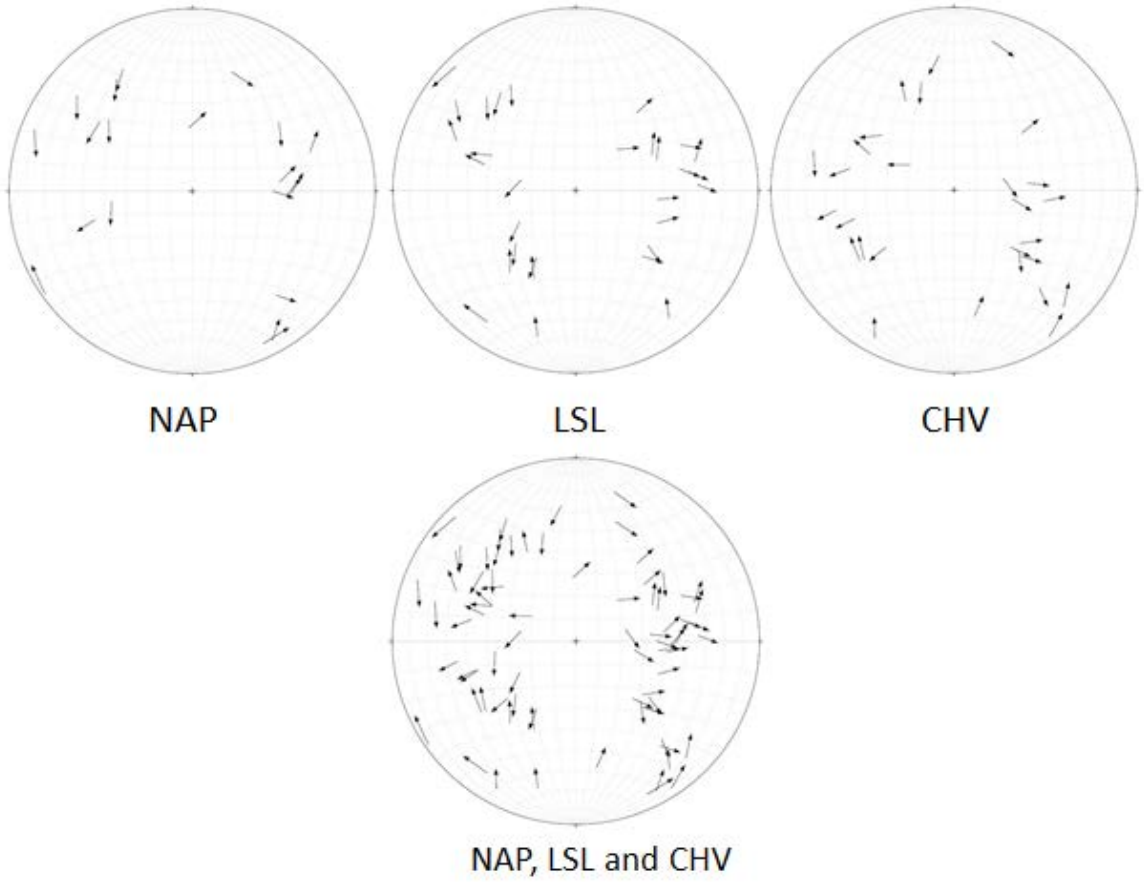

Figure 4.13: Tangent lineation plots for Northern Appalachian (NAP), Lower St. Lawrence (LSL) and Charlevoix (CHV) regions showing $\sigma_1 = \sigma_2$ and σ_3 oriented horizontally. The data have been rotated 90° clockwise for comparison and σ_3 in the area is actually vertical. (Created using FaultKin v.5.2.6)

Fig. 4.13 shows σ_3 oriented horizontally. The data have been rotated 90° clockwise for comparison with figure 4.12 and the σ_3 in the area is actually vertical.

4.6 Resolved shear stress

The kinematic data obtained so far were used to make a first-order estimate of resolved shear stresses along the 2 principal fault systems (a) St Lawrence fault (025/ 65) and (b) Oak bay fault (150/90). The forces were calculated from the earthquake energy (Appendix 1, Mo), the orientation of principal stresses for each area (Fig. 4.14c, and Fig 4.15c) and the stress ratio was

estimated from the stress inversion which indicates ϕ ~1. A dimensionless Mohr diagram was constructed to show the 3-D state of stress over the CHV (Fig. 4.14b) and NAP (Fig. 4.15b) regions shows the Mohr diagram which indicates the normal and shear stress acting on all slip planes in the study area.

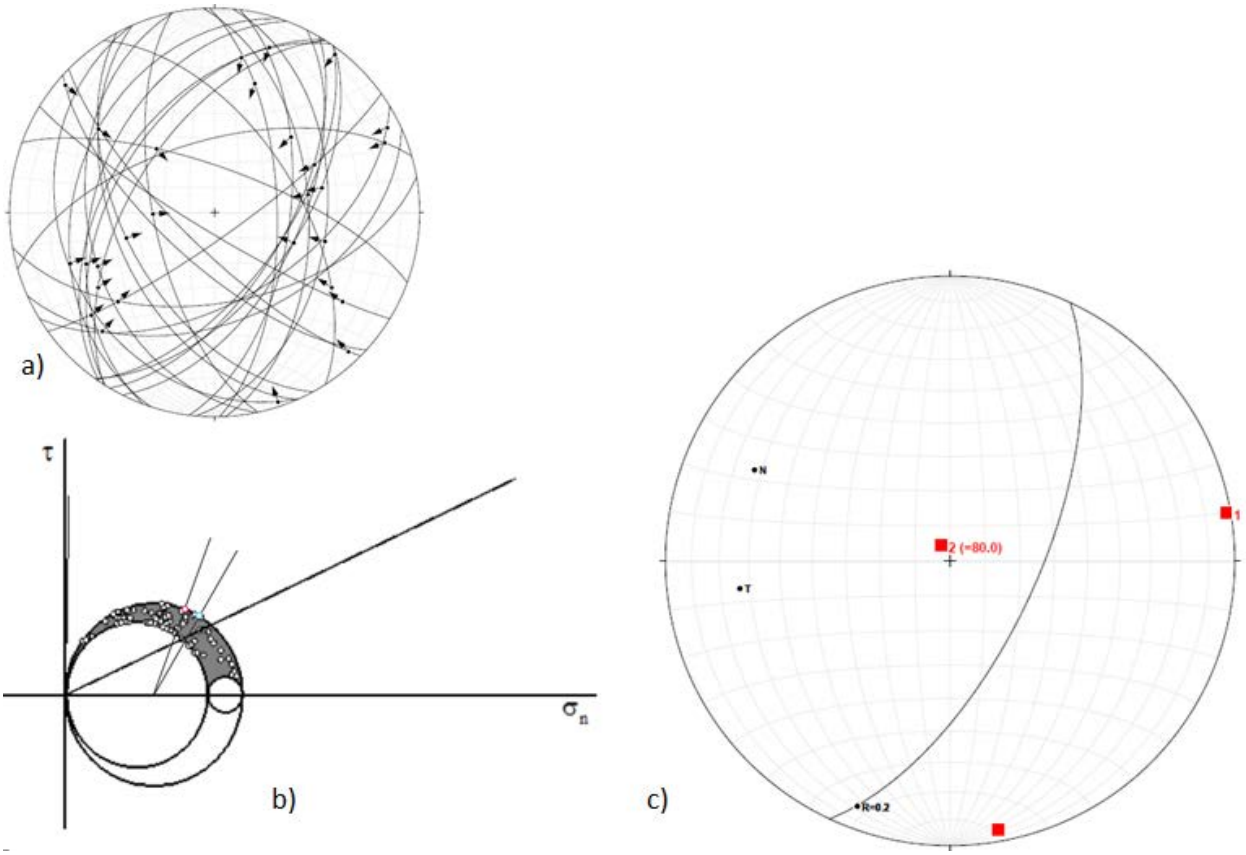

Figure 4.14: (a) Charlevoix faults and their hanging wall slip direction (b) Dimensionless Mohr diagram for showing both St. Lawrence (red) and Oak Bay faults (blue). The large contained circle represents the relative magnitude of $\sigma_3\sigma_2$, the small contained circle represents the relative magnitude of $\sigma_1\sigma_2$ where the largest circle, the containing circle, is $\sigma_3\sigma_1$. (c) Calculated kinematic axes showing σ_1, σ_2, and σ_3 in red squares as well as N, normal stress, T, traction stress and R, shear stress.

The Mohr diagram in Fig. 4.14 (b) shows that σ_2 and σ_1 are close to equal and σ_3 is much smaller. Normalising the diagram to σ_3 =0 and σ_1 =1 yields σ_2= 0.8 σ_1. This stress field is most

similar to the stress ellipsoid obtained by tangent lineation analysis (Fig. 4.12d) where $\sigma_1 \approx \sigma_2$ and $\phi \approx 1$.

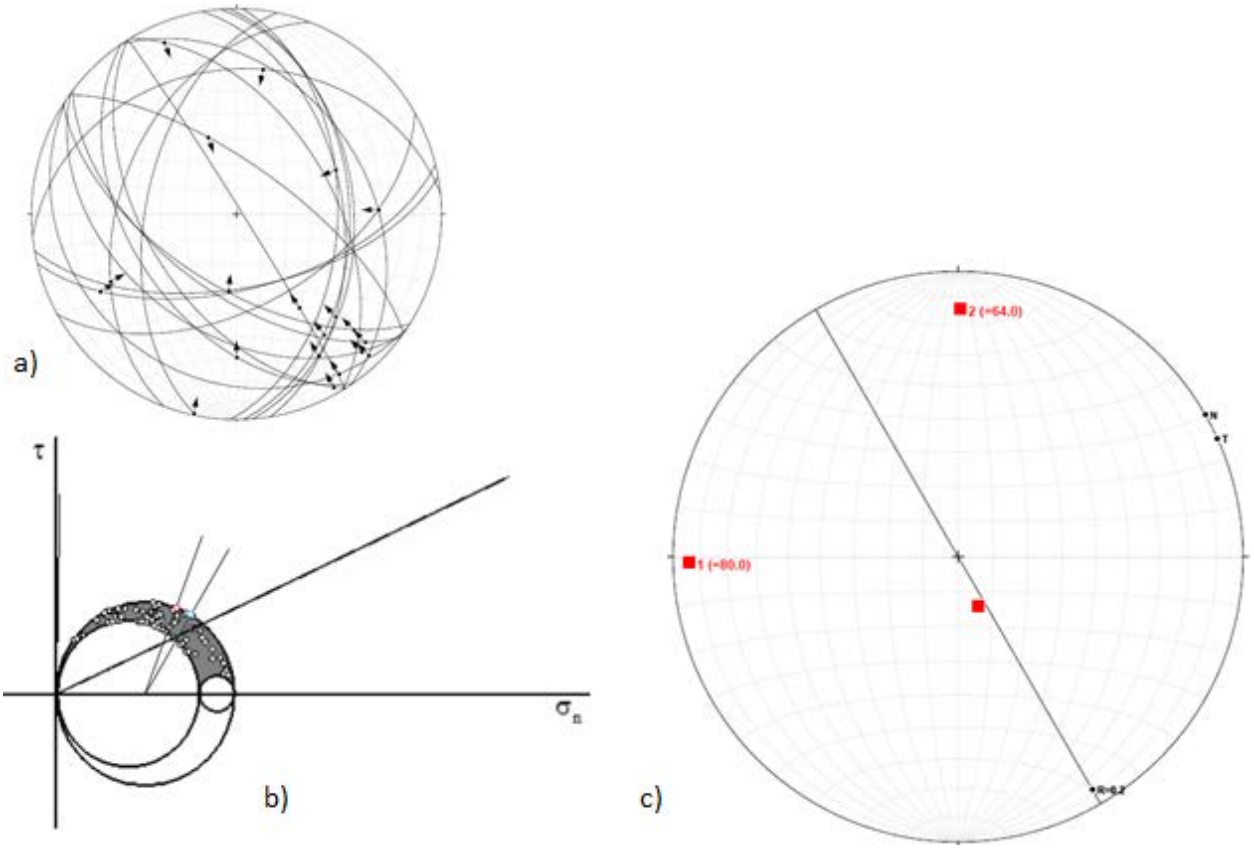

Figure 4.15: (a) Northern Appalachian faults and their hanging wall slip direction (b) Dimensionless Mohr diagram showing both St. Lawrence (red) and Oak Bay faults (blue). The large contained circle represents the relative magnitude of $\sigma_3\sigma_2$, the small contained circle represents the relative magnitude of $\sigma_1\sigma_2$ where the largest circle, the containing circle, is $\sigma_3\sigma_1$. . (c) Calculated kinematic axes showing σ_1, σ_2, and σ3 in red squares as well as N, normal stress, T, traction stress and R, shear stress.

The Mohr diagram in figure 4.15b shows again that σ_2 and σ_1 are close to equal and σ_3 is much smaller. Normalising the diagram to $\sigma_3 = 0$ and $\sigma_1 = 1$ yields the same stress ratio as the St. Lawrence fault: $\sigma_2 = 0.8\,\sigma_1$. This stress field is most similar to the stress ellipsoid obtained by tangent lineation analysis (Fig. 4.12d) where $\sigma_1 \approx \sigma_2$ and $\phi \approx 1$.

Using these parameters, the calculations in table 2 were found for the St. Lawrence and Oak Bay faults.

Table 2: Calculations from stress inversion

Parameter	**St. Lawrence fault**	**Oak Bay fault**
Orientation of the principal stresses (trend/plunge)	(080.3/01.7) σ_1 (170.5/05.1) σ_2 (332.2/84.6) σ_3	(268.7/05.5) σ_1 (000.0/13.9) σ_2 (157.6/75.0) σ_3
Ratio of the magnitude of principal stresses (R)	0.2	0.2
Orientation of the fault plane (strike/dip)	(025/65)	(150/90)
Traction	82.59543	76.37438
Resolved stresses (σ_n)	72.08245	76.01671
Resolved stresses ($\sigma_{s)}$	40.32523	7.382813

On the Oak Bay fault, the magnitude of shear stress is one order of magnitude lower than the normal stress (Fig. 4.15c) which makes reactivation of the Oak Bay fault plane highly unlikely. The relative orientation between σ_1 and the fault plane (Fig. 4.15b) indicates that if it were reactivated it would likely be a sinistral strike-slip fault. Of the faults in the CHV area (Fig. 4.14a), four or five have a similar orientation to the St. Lawrence fault (Fig. 4.14c) meaning that they may be reactivated occasionally but, the majority of active faults in the CHV area are not aligned with the St. Lawrence fault (Fig 4.14a).

4.7 Seismic hazard at Point Lepreau

Seismic hazard at Point Lepreau's nuclear generating station has been a concern for a long time. In the past, all criteria used to assess the hazard were based on the Oak Bay fault (Connell, King's County Record). This study has analysed the shear stress on two faults; the Oak Bay fault and the St. Lawrence fault and found that the Oak Bay fault is not a likely risk to Point

Lepreau as the shear stress is about ten times less than the normal stress. The St. Lawrence fault is reactivated on occasion but is unlikely to cause severe damage to Point Lepreau's generating station. Other risks studied in this paper include reactivation of other faults (such as the Cobequid-Chedabucto Fault Zone), and earthquake generated tsunamis.

The 1929 Mn=7.2 event caused a submarine landslide that displaced approximately $10^{11}m^3$ of sediment that extended as far as 250 km away from the epicentre (Bent, 1995). The displacement of this material caused a tsunami that ruptured 12 transatlantic cables, killed 27 people (Bent, 1995) and reached as far as Maine (Fig. 14.16); effects were even felt in Hudson Bay (Fig. 4.16). Seismicity in the Laurentian Channel region consists of two or three earthquake clusters (Bent 1995); each is trending NW-SE and are parallel to each other. The 1929 earthquake was the largest recorded in eastern Canada and the most harmful as well. The harm stemmed mostly from the tsunami that resulted from the earthquake-generated landslide (Bent, 1995). Although it is unlikely that the slope will fail again soon due to the lack of sediment build up in the LSP zone (Bent, 1995) for much larger earthquakes or earthquakes with different regimes from those of the 1929 and 1975 earthquakes, tsunamis cannot be completely ruled out (Bent, 1995). In addition to this, the 1975 event on the LSP was a thrust event therefore, a potential for a large thrust earthquake to occur cannot be ruled out either.

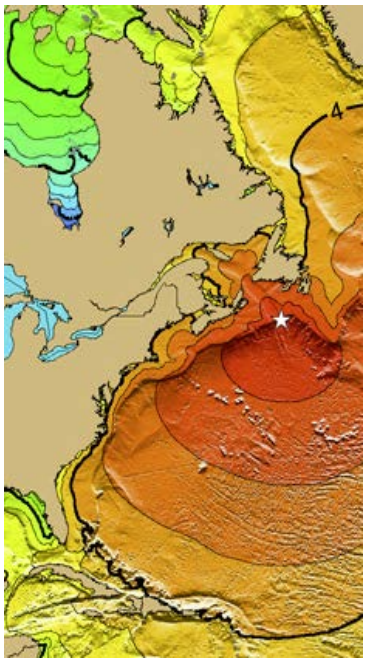

Figure 4.16: Tsunami effects after the1929 Mn=7.2 earthquake. Star shows the epicentre of earthquake, and contours are in hours and show when the tsunami effects were felt over eastern Canada in relation to the epicentre (Image adapted from National Oceanic and Atmospheric Administration's Satellite and Information Service).

The 1929 event took ~4 hours to reach Point Lepreau. Four hours should be adequate for most nuclear generating stations to prepare for a tsunami and it also provides time for the tsunami waves to attenuate. The fact that the nuclear generating station in Point Lepreau received a new five-year operation license in February, 2012 (Patterson, 2012), indicates that the site's safety regulations are up to par.

This area is understudied and there are many opportunities for future work which include: investigating the effect of peripheral bulge due to isostatic rebound on seismicity in the study area, analysing the shear stress on other faults within the study area, comparison of seismic data to fault plane solutions, investigation of the cause of earthquakes in the Grand Banks region, investigation into the rate of sediment build-up on the Laurentian Slope, tsunami propagation and probability of channeling of a tsunami through the Bay of Fundy.

References

Adams, J. , Sharp, J., & Stagg, M. C. (1988). *New focal mechanisms for southeastern canadian earthquakes.* Open File 1892. Geologic Survey of Canada.

Adams, J. (1991). *New focal mechanisms for eastern canada* Open File 2430. Geologic Survey of Canada.

Adams, J., Vonk, A., Pittman, D., & Vatcher, H. (1989). *New focal mechanisms for southeastern canadian earthquakes - volume II.* Open File 1995. Geological Survey of Canada.

Allmendinger, R. W. (2011). *FaultKin* (5.2.6 ed.)

Allmendinger, R. W. (2011, 2012). *Stereonet version 7.2.3*

Bent, A. L. (1995). A complex double-couple source mechanism for the ms 7.2 1929 grand banks earthquake. *Bulletin of the the Seismological Society of America, 85*, 1003-1020.

Bent, A. L., & Drysdale, J. (2000). *Focal mechanisms for eastern canadian earthquakes: 1 july 30-31 december 1998*. Open File 3870. Geologic Survey of Canada.

Bent, A. L., & Drysdale, J. (2002). *Focal mechanisms for eastern canadian earthquakes of 2000* Open File 4289. Geologic Survey of Canada.

Bent, A. L., & Perry, C. (1999). *Focal mechanisms for eastern canadian earthquakes: 1 january 1996 - 30 june 1998*. Open File 3698. Geologic Survey of Canada.

Brent, A. L., & Perry, H. K. C. (2001). *Focal mechanisms for eastern Canadian earthquakes:1994-1995.* Open File 4088. Geologic Survey of Canada.

Connell, M. Previously unconsidered chedabucto fault: Geologist charges Point Lepreau in earthquake hazard. *King's County Record, Sussex, NB,*

Craymer, M.R., J. Henton, M. Piraszewski, E. Lapelle. (2011). An updated GPS velocity field for canada. *Eos Transactions, American Geophysical Union, AGU, 92(51), Fall Meeting Supplement, Abstract G21A-0793, 2011*(51).

Eisbacher, G. H. (1969). Displacement and stress field along part of the Cobequid Fault, Nova Scotia. *Canadian Journal of Earth Sciences, 6,* 1095-1098.

Fossen, H. (2010). *Structural Geology*, pp.80-81, 89-92, 190-198. Cambridge University Press, Cambridge, UK.

Gobeil, J.P., Pe-Piper, G. & Piper, D. (2006). The West Indian road pit, central Nova Scotia: Key to the early Cretaceous Chaswood formation. *Canadian Journal of Earth Science, 43,* 391-403.

Heidbach, O., Tingay, M., Barth, A., Reinecker, J., Kurfeß, D. and Müller, B. (2008). *The world stress map database release*

IRIS. (2012). *GPS—Measuring plate motion: How fast are the tectonic plates moving?* Retrieved March/18, 2012,
from http://www.iris.edu/hq/files/programs/education_and_outreach/aotm/14/1.GPS_Background.pdf

Leblanc, G. & Klimkiewicz, G. C. (1994). *Seismological issues: History and examples of earthquake hazard assessment for Canadian nuclear generating stations.* Open file 2929. Geologic Survey of Canada.

Macinnes, E.A. & White, J.C. Geometric and kinematic analysis of a transpression terrane boundary: Minas fault system, Nova Scotia, Canada.

Mawer, C.K. & White, J.C. (1987). Sense of displacement on the Cobequid-Chedabucto Fault system, Nova Scotia, Canada *Canadian Journal of Earth Science, 24*, 217-223.

Mazzotti, S. &. T., J. (2010). State of stress in central and eastern North American seismic zones. *Lithosphere, 2*(2), 76-83.

Miller, B.V., Barr, S.M., Black, R.S. (2007). Neoproterozoic and Cambrian U–Pb (zircon) ages from Grand Manan island, New Brunswick: Implications for stratigraphy and northern appalachian terrane correlations. *Canadian Journal of Earth Sciences, 44*(7), 911-923.

Natural Resources Canada. (2011). *Earthquake activity in New Brunswick.* Retrieved 03/12, 2012, from http://www.earthquakescanada.nrcan.gc.ca/zones/NASZ/nbrunswick-eng.php

Natural Resources Canada. (2011). *Search the earthquake database: National earthquake database.* Retrieved November/6, 2011, from http://earthquakescanada.nrcan.gc.ca/

Patterson, B. (2012). *WIN: Point Lepreau must update earthquake risk assessment testing.* Retrieved March/18, 2012, from http://canadians.org/blog/?p=13663

Pe-Piper, G. & Piper, D. (2004). The effects of strike-slip motion along the Cobequid – Chedabucto – Southwest Grand banks Fault system on the Cretaceous–Tertiary evolution of Atlantic Canada. *Canadian Journal of Earth Science, 41*, 799-808.

Sample, I. (2011, Sunday 13 March). Japan's nuclear fears intensify at two Fukushima power stations. *The Guardian.*

Smith, R. B. (2000). *Interpretations of fault plane solutions.* Retrieved March/18, 2012, from http://www.uusatrg.utah.edu/RBSMITH/public_html/TEACHING/GG554/notes/20Note/20-4.pdf

Tremblay, A. & Lemieux, Y. (2001). *Supracrustal faults of the St. Lawrence Rift system between Cap-Tourmente and Baie-Sainte-Paul, Quebec.* Geologic Survey of Canada: Current Research.

U.S. Geological Survey. (2009). *Earthquake glossary- earthquake hazard.* Retrieved 11/6, 2011, from http://earthquake.usgs.gov/learn/glossary/?termID=64

U.S. Geological Survey. (2009). *Earthquake hazards program: Seismic properties of north america and the surrounding ocean basins.* Retrieved March/18, 2012, fromhttp://earthquake.usgs.gov/research/structure/crust/nam.php

U.S. Geological Survey. (2009). *FAQs- measuring earthquakes.* Retrieved Feb/22, 2012, from http://earthquake.usgs.gov/learn/faq/?categoryID=2&faqID=33

U.S. Geological Survey. (2010). *Earthquake hazards program: Focal mechanisms.* Retrieved 11/6, 2011, from http://earthquake.usgs.gov/learn/topics/beachball.php

U.S. Geological Survey. (2010). *Earthquake search: Magnitudes.* Retrieved Feb/22, 2012, from Page URL: http://earthquake.usgs.gov/earthquakes/eqarchives/epic/code_magnitude.php

U.S. Geological Survey. (2011). *ShakeMap scientific background: Map types- peak acceleration maps.* Retrieved 11/ 6, 2011, from http://earthquake.usgs.gov/earthquakes/shakemap/background.php

Wildish, D.J., Akagi, H.M., McKeown, D.L., Pohle, G.W. (2008). Pockmarks influence benthic communities in Passamaquoddy Bay, bay of fundy, canada. *Marine Ecology Progress Series, 357*, 51-66.

World Nuclear Association. (2012). *Uranium in canada.* Retrieved 03/11, 2012, from http://www.world-nuclear.org/info/inf49.html

WSM Database. (2009). *Detailed explanation of the data record fields.* Retrieved 03/16, 2012, from http://dc-app3-14.gfz-potsdam.de/pub/stress_data/stress_data_frame.html

Appendix I: Data

Source Event name	**Latitude (N)**	**Longitude (W)**	**Best Sol'n Strike**	**Best Sol'n Dip**	**Best Sol'n Rake**	**Mn**	**Seismic Zone**	**Depth (km)**	**Mo (dyne*cm)**
Open file 2430									
880102	47.41N	70.44W	133	44	60	3.6	CHV	12	2.81838E+21
			351	53	115				
880128	48.0N	65.67 W	120	81	3	3.9	NAP	18	7.94328E+21
			30	87	171				
880313	47.44N	70.38 W	183	25	35	3.1	CHV	7	5.01187E+20
			60	76	111				
880512	47.03N	70.82W	297	51	77	3.1	CHV	14	5.01187E+20
			137	41	105				
881123	48.13N	71.2W	343	48	82	4.7	LSL	29	1.25893E+23
			175	42	99				
881125	48.13N	71.21 W	326	67	55	6.5	LSL	29	6.30957E+25
			207	42	143				
881126	48.14N	71.30 W	339	46	103	4.1	LSL	26	1.58489E+22
			141	46	77				
890309	47.72N	69.86W	168	31	71	4.3	CHV	10	3.16228E+22
			11	60	102				

890311	47.72N	69.87W	184	38	80	4.4	CHV	10	4.46684E+22
			17	52	98				
871206	47.82N	69.96 W	130	65	79	3	CHV	20	3.54813E+20
			335	27	113				
Open file 1892	49.84N	68.62W	58.6	71	69	No data	LSL	No data	No data
			23.2	28	137				
			19.9						
800403	48.71N	67.81W	75	56	53	4.1	LSL	18	1.58489E+22
			0.1	48	132				
			15						
830117	48.99N	67.21W	80	53	65	4.1	LSL	17	1.58489E+22
			0	44	129				
			10						
840329	49.61N	66.45W	87.5	50	83	3.2	LSL	18	7.07946E+20
			0.1	40	98				
			2.5						
840411	49.31N	67.51W	80.1	57	66	3.8	LSL	18	5.62341E+21
			0	40	122				
			9.9						
840528	49.61N	66.35W	79.8	57	66	3.2	LSL	18	7.07946E+20
			0.1	40	122				
			10.2						
840923	46.00N	64.88W	72.3	78	54	3.6	NAP	12	2.81838E+21
			0.1	38	160				
			17.7						
850412	45.37N	70.69W	85	41	75	3.5	NAP	7	1.99526E+21
			0	51	103				

			5						
850816	49.26N	67.60W	52.9	85	-14	3.2	LSL	18	7.07946E+20
			2.2	76	-175				
			37.1						
860111	47.70N	70.11W	77.6	59	60	4	CHV	5	1.12202E+22
			0.2	42	129				
			12.3						
860509	46.54N	66.15W	72.5	62	49	3.3	NAP	11	1E+21
			0.1	48	141				
			17.5						
860919	47.30N	70.32W	84.9	46	76	4.2	CHV	22	2.23872E+22
			0	46	104				
			5.1						
861109	49.25N	67.39W	80	53	65	4.2	LSL	18	2.23872E+22
			0	44	120				
			27.3	83	130				
			39.3						
OF 1995									
740609	47.343	70.24	23.2	73	42	1.8	CHV	10	5.62341E+18
			19.9	50	157				
740623	47.51	70.22	75	45	90	1.5	CHV	15	1.99526E+18
			0.1	45	90				
850325	47.74	69.69	15	67	20	2.9	CHV	28	2.51189E+20
			80	71	156				
861017	47	66.54	0	67	46	4.1	NAP	5	1.58489E+22
			10	48	149				
870318	47.72	70.19	87.5	55	60	3.3	CHV	4	1E+21
			0.1	45	125				
870503	48.74	68.25	2.5	54	37	3.6	LSL	14	2.81838E+21

			80.1	60	138				
870617	48.87	68.71	0	61	73	3	LSL	14	3.54813E+20
			9.9	33	118				
870806	49.61	66.98	79.8	64	56	3.3	LSL	18	1E+21
			0.1	41	139				
880424	46.03	64.9	10.2	59	54	3.7	NAP	4	3.98107E+21
			72.3	46	134				
OF 3870			0.1						
980715	47.02	66.61	17.7	67	112	4	NAP	5	1.12202E+22
			85	32	49				
981022	49.34	66.82	0	30	58	4.1	LSL	18	1.58489E+22
			5	67	107				
OF 3698			52.9						
971028	47.67	69.9	2.2	82	37	4.7	CHV	12.32	1.25893E+23
			37.1	53	169				
980317	43.75	56.38	77.6	40	11	4.4		18	4.46684E+22
			0.2	83	130				
OF 4088			12.3						
940714	47	66.6	72.5	79	33	4.1	NAP	5	1.58489E+22
			0.1	57	167				
OF 4289			17.5						
712	47.56	71.07	84.9	47	70	4.2	CHV	10	2.23872E+22
			0	47	111				
Global CMT Catalog									
010982A NEW BRUNSWICK	46.87	66.41	324	47	42	5.5	NAP	10	1.94E+24
			202	61	129				
011182B	47.24	66.44	190	44	121	5	NAP	15	3.93E+23

NEW BRUNSWICK									
			329	53	63				
112588C SOUTHERN QUEBEC	48.01	71.17	189	39	135	5.8	NAP	27.5	6.88E+24
			317	64	60			5.9	